

# A Mountaineering Strategy to Excited States: Highly-Accurate Energies and Benchmarks for Bicyclic Systems

Pierre-François Loos<sup>\*,†</sup> and Denis Jacquemin<sup>\*,‡</sup>

<sup>†</sup>Laboratoire de Chimie et Physique Quantiques, Université de Toulouse, CNRS, UPS, France

<sup>‡</sup>Université de Nantes, CNRS, CEISAM UMR 6230, F-44000 Nantes, France

E-mail: loos@irsamc.ups-tlse.fr; Denis.Jacquemin@univ-nantes.fr

## Abstract

Pursuing our efforts to define highly-accurate estimates of the relative energies of excited states in organic molecules, we investigate, with coupled-cluster methods including iterative triples (CC3 and CCSDT), the vertical excitation energies of 10 bicyclic molecules (azulene, benzoxadiazole, benzothiadiazole, diketopyrrolopyrrole, fuofuran, phthalazine, pyrrolopyrrole, quinoxaline, tetrathiafulvalene, and thienothiophene). In total, we provide *aug-cc-pVTZ* reference vertical excitation energies for 91 excited states of these relatively large systems. We use these reference values to benchmark various wave function methods, i.e., CIS(D), EOM-MP2, CC2, CCSD, STEOM-CCSD, CCSD(T)(a)\*, CCSDR(3), CCSDT-3, ADC(2), ADC(2.5), ADC(3), as well as some spin-scaled variants of both CC2 and ADC(2). These results are compared to those obtained previously on smaller molecules. It turns out that while the accuracy of some methods is almost unaffected by system size, e.g., CIS(D) and CC3, the performance of others can significantly deteriorate as the systems grow, e.g., EOM-MP2 and CCSD, whereas others, e.g., ADC(2) and CC2, become more accurate for larger derivatives.

## 1. INTRODUCTION

Reference sets encompassing accurate experimental and/or theoretical data have always enjoyed a high popularity in the electronic structure community. Indeed, these allow for rapid and fair comparisons between theoretical models for properties of interest. The pioneering reference sets are likely the so-called Gaussian-*x* databases originally collected by Pople and collaborators 25 years ago and constantly extended since then.<sup>1-5</sup> These datasets contain a large number of experimental reference values (atomization energies, bond dissociation energies, etc) and remain popular today to assess the performances of new exchange-correlation functionals (see, for example, Ref. 6) within density-functional theory (DFT) as well as higher-level methods.<sup>7-9</sup> Many other sets collecting reliable experimental and/or theoretical values have been developed throughout the years. The panel is so wide that being exhaustive is beyond reach, but we can cite: (i) the S22 and S66 benchmark sets of interaction energies for weakly-bound systems;<sup>10,11</sup> (ii) the HEAT set collecting high-accuracy theoretical formation enthalpies;<sup>12</sup> (iii) the *GW*100 and *GW*5000 sets of ionization energies;<sup>13,14</sup> and (iv) the very extended GMTKN<sub>xy</sub> thermochemical and kinetic databases proposed by Goerigk and Grimme.<sup>15-17</sup> In this framework, one can certainly also pinpoint the successes of Barone’s group in deriving very accurate “semi-experimental” structural, rotational, and vibrational reference parameters for a large panel of molecules of various sizes.<sup>18-20</sup>

Since 2018, our groups have made joint efforts to produce highly-accurate energies of electronically excited states (ESs)

in molecular systems,<sup>21-25</sup> in line with the earlier contributions from the Mulheim group.<sup>26-28</sup> Our key results were recently collected in the so-called QUEST database,<sup>29</sup> that contains more than 500 theoretical best estimates (TBEs) of vertical transition energies (VTEs) computed in small- and medium-sized organic molecules with Dunning’s *aug-cc-pVTZ* basis set. For the smallest systems (1–3 non-hydrogen atoms),<sup>21,24</sup> most VTEs are of full configuration interaction (FCI) quality and they have been computed with the *Configuration Interaction using a Perturbative Selection made Iteratively* (CIPSI) method.<sup>30-35</sup> For the molecules containing 4 non-hydrogen nuclei,<sup>23</sup> most reference values are derived from basis-set-extrapolated coupled-cluster (CC) calculations including contributions from the singles, doubles, triples, and quadruples (CCSDTQ).<sup>36</sup> Finally for the larger systems,<sup>24,29</sup> CC with singles, doubles, and triples (CCSDT)<sup>37-41</sup> values are employed to define the TBEs, typically by computing the CCSDT excitation energies with a double- $\zeta$  basis set and correcting for basis set effects thanks to VTEs determined with the corresponding approximate third-order CC (CC3) model.<sup>42,43</sup>

The original QUEST database contains a reasonably broad panel of organic and inorganic molecules (closed- and open-shell compounds, cyclic and linear systems, pure hydrocarbons, heteroatomic structure, etc) and ESs (valence and Rydberg transitions, singlet, doublet, and triplet excitations, with or without a significant double excitation character, etc) but it clearly lacked charge-transfer (CT) excitations, an aspect that we have recently corrected.<sup>25</sup> As the VTEs

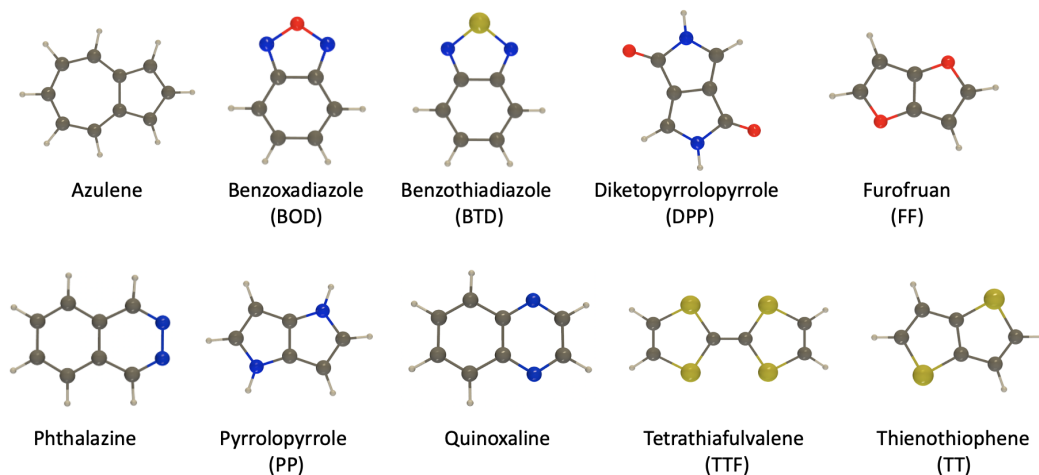


Figure 1: Representation of the investigated derivatives.

cannot be measured experimentally, but are the “simplest” ES property to compute, the QUEST database is especially useful for performing cross-comparisons between computational models.<sup>44</sup> As examples, the VTEs included in QUEST and their corresponding TBEs have allowed us and others to (i) clearly determine the relative accuracies of CC3 and CCSDT-3;<sup>21,23</sup> (ii) unambiguously define the performance of ADC(3);<sup>45</sup> (iii) assess the fourth-order approximate CC approach (CC4) compared to its CCSDTQ parent;<sup>46</sup> and (iv) benchmark hybrid and double-hybrid exchange-correlation functionals<sup>47-51</sup> as well as orbital-optimized excited-state DFT calculations.<sup>52</sup>

Understandably, most molecules included in QUEST are rather compact. To date, only four molecules from the QUEST dataset contain 8 non-hydrogen atoms or more: octatetraene, the highly-symmetric ( $D_{2h}$ ) benzoquinone, naphthalene, and tetra-azanaphthalene.<sup>29</sup> For comparison, QUEST includes 20 (10) molecules containing 4 (6) non-hydrogen nuclei.<sup>29</sup> There is a clear imbalance here, and the present contribution is a step towards correcting this bias by providing TBEs for a large number of ESs for the ten compounds sketched in Figure 1 which encompass from 8 to 10 non-hydrogen atoms. These ten compounds have been selected to be of chemical interest with many building blocks used as chromophores in real-life dye chemistry. As we detail below, beyond extending the QUEST database, the present work also provides, for the vast majority of ESs considered, what can likely be viewed as the most accurate VTEs to date for these systems. Consequently, the data collected here can also be of interest for more specific studies, e.g., for choosing an appropriate exchange-correlation functional for studies focussing on optimizing the absorption properties of diketopyrrolopyrroles.

## 2. COMPUTATIONAL DETAILS

We closely follow the computational protocols used in our previous works,<sup>21-25,29,45</sup> which is briefly summarized below. Note that all calculations are performed within the frozen-core approximation.

The ground-state geometries are optimized at the CC3 level<sup>42,43</sup> with the cc-pVTZ basis set using CFOUR2.1.<sup>53</sup>

These optimizations are achieved in a Z-matrix format, so that point group symmetry ( $C_{2v}$ ,  $C_{2h}$ , or  $D_{2h}$ ) is strictly enforced. Default convergence parameters are applied. Cartesian coordinates are provided in the Supporting Information (SI) for all molecules treated here. These geometries are next used to compute VTEs with CC methods. Note that, in the following, we do not specify the EOM (equation-of-motion) or LR (linear-response) prefix in the CC schemes as the two formalisms deliver the same transition energies (yet different properties).

In a first step, we perform CCSD/*aug-cc-pVTZ* calculations<sup>54-58</sup> for the 6–20 lowest-energy ESs of all molecules considering both the singlet and triplet manifolds. The main purpose of these calculations, performed with GAUSSIAN 16,<sup>59</sup> is to screen the various ESs and identify the key molecular orbitals (MOs) associated with these transitions (extended data are given in the SI for all molecules). The specific nature of these ESs is determined by examining these MOs, which allows us, in the vast majority of the cases, a straightforward identification of the Rydberg and valence transitions. For the latter, we also perform ADC(2)/*aug-cc-pVTZ*<sup>60,61</sup> calculations using Q-CHEM 5.3/5.4,<sup>62</sup> as well as TD-CAM-B3LYP/*aug-cc-pVTZ*<sup>63</sup> calculations with GAUSSIAN,<sup>59</sup> in an effort to estimate the CT character of the valence ESs. Following Ref. 25, we consider two CT metrics: (i) the electron-hole distance as determined from the ADC(2) transition density matrix,<sup>64,65</sup> and (ii) the CT distance as obtained with CAM-B3LYP applying the well-known Le Bahers’ model.<sup>66,67</sup> As detailed elsewhere,<sup>25</sup> although these two metrics often yield rather consistent estimates of the CT strength, there is no definitive definition of CT state. We consider that a given transition has a non-negligible CT character if the electron-hole distance provided by these metrics is greater than 1 Å.

In a second stage, we apply CC3<sup>42,43</sup> to estimate the VTEs of selected ESs with three atomic basis sets, namely 6-31+G(d), *aug-cc-pVDZ*, and *aug-cc-pVTZ*. These calculations are carried out with either CFOUR,<sup>53</sup> and/or DALTON 2018,<sup>68</sup> the latter being able to provide CC3 triplet transitions. For all tested cases, the two codes provide the same

VTEs within  $\pm 0.001$  eV. When the CC3/*aug-cc-pVTZ* calculations were achievable with Dalton, we provide below  $\%T_1$ , that is, the percentage of single excitations involved in a given transition at this level of theory. Consistent with earlier works,<sup>21,22,26</sup>  $\%T_1$  is typically much larger for triplet transitions than for their singlet counterparts, the latter having a larger contributions from double excitations. This is why, for all singlet ESs considered herein, we also report CCSDT<sup>37-41</sup> excitation energies (computed with CFOUR<sup>53</sup>) obtained with at least one of the two double- $\zeta$  basis sets, the difference between the CC3 and CCSDT VTEs providing a first hint at the convergence of the VTEs with respect to the maximum excitation degree of the truncated CC series. Of course, neither CC3 nor CCSDT transition energies can be considered as of FCI quality. Thus, one can certainly wonder what would be the impact of ramping up further the truncation degree of the CC expansion. However, given the size of the molecules treated here, such task is very clearly beyond computational reach. Besides, we wish to stress that, for most of the molecules depicted in Figure 1, the present CC3 and CCSDT VTEs are the first being published. Indeed, as detailed in the next Section, all previous efforts typically consider significantly lower levels of theory.

In a third phase, we assess the performances of many wave function methods using these new TBEs. All these benchmark calculations employ the *aug-cc-pVTZ* basis set. Consistent with the QUEST database,<sup>29</sup> we test: CIS(D),<sup>69,70</sup> EOM-MP2,<sup>71</sup> CC2,<sup>72,73</sup> CCSD,<sup>54-58</sup> STEOM-CCSD,<sup>74,75</sup> CCSD(T)(a)\*,<sup>76</sup> CCSDR(3),<sup>77</sup> CCSDT-3,<sup>78,79</sup> CC3,<sup>42,43</sup> ADC(2),<sup>60,61</sup> ADC(3),<sup>61,80,81</sup> and ADC(2.5).<sup>45</sup> The ADC(2), ADC(3), and EOM-MP2 calculations are performed with Q-CHEM,<sup>62</sup> using the resolution-of-the-identity (RI) approximation and tightening the convergence and integral thresholds. Note that the ADC(2.5) VTEs are the simple average of the ADC(2) and ADC(3) values. The CIS(D) and CCSD VTEs are obtained with GAUSSIAN,<sup>59</sup> CC2 and CCSDR(3) results are obtained with DALTON,<sup>68</sup> whereas CCSD(T)(a)\* and CCSDT-3 energies are computed with CFOUR.<sup>53</sup> STEOM-CCSD calculations are carried out with ORCA 4.2.1<sup>82</sup> and we report only ESs for which the active character percentage is larger than 98%. In addition, we also evaluate the spin-component scaling (SCS) and scaled spin-opposite (SOS) CC2 approaches, as implemented in TURBOMOLE 7.3.<sup>83,84</sup> For ADC(2), we apply two distinct sets of SOS parameters, the ones available in Q-CHEM<sup>85</sup> and the ones proposed by TURBOMOLE.<sup>83</sup>

### 3. RESULTS AND DISCUSSION

#### 3.1 Reference values

##### 3.1.1 Azulene

The ESs of this isomer of naphthalene were investigated in several theoretical works,<sup>25,86-92</sup> and we have considered here six singlet ESs (four valence, two Rydberg) and four triplet ESs (all valence). We refer the interested reader to Table 1 as well as the SI for further details regarding oscillator strengths and involved MO pairs. The four valence singlet ESs are consistently attributed by experimental<sup>91,93-96</sup> and theoretical<sup>87-91</sup> approaches. For their Rydberg counterparts, the assignments are clearly more challenging (see below).<sup>90,96</sup>

According to the analysis of the CT strengths presented in our earlier work,<sup>25</sup> two ESs present a mild CT character with an electron-hole separation around 1 Å. For these two states, the present work is, as far as we are aware, the first to present CC results including iterative triples for azulene.

For the singlet transitions, the variations between CCSDT/6-31+G(d) and CC3/6-31+G(d) are very mild (roughly  $\pm 0.02$  eV) except for the second  $A_1$  ES for which a slightly larger effect can be noticed (+0.04 eV). In the same vein, the basis set effects are following the expected trends, with maximal variations of approximately 0.07 eV between the *aug-cc-pVDZ* and *aug-cc-pVTZ* singlet VTEs at the CC3 level. There is therefore a high level of consistency between the various values collected in Table 1.

There are several measurements of the optical properties of azulene performed with diverse experimental techniques,<sup>91,93-96</sup> some of which are summarized at the right-hand-side of Table 1. Let us start with the singlet transitions. Our VTE for the lowest  $^1B_2$  is significantly below the measured 0-0 energy, by approximately  $-0.4$  eV. We recall that this is actually the expected trend: the vertical energies do not account for the geometric relaxation in the ES, nor the difference of zero-point vibrational energies of the two states, and should therefore exceed their 0-0 counterparts.<sup>86,97</sup> The same trend pertains for all higher-energy valence transitions with typical shifts going from  $-0.3$  to  $-0.5$  eV between the VTEs listed in Table 1 and the experimental values. For the two Rydberg ESs, attributing the two lowest experimental peaks to the two lowest theoretical Rydberg ESs, one obtains trends that are not incompatible with the measurements. Yet, one should clearly be very cautious and more experimental and theoretical analyses would be welcome for these particular ESs. For the triplets transitions, our estimates are slightly (for the two  $^3A_1$  states) or significantly (for the two  $^3B_2$  states) larger than the measurements but provide the same ranking.

As compared to the first CASPT2 values published almost two decades ago,<sup>87</sup> our CC3/*aug-cc-pVTZ* values are similar for the  $^1A_1$  VTEs, but higher for the  $^1B_2$  excitations. If one compares to the previous high-level CC estimates including perturbative triples corrections (and performed with relatively compact basis sets),<sup>88,90</sup> one notes that the present energies are slightly lower/higher than the CCSDR(3) values of Ref. 88 for the valence/Rydberg transitions, whereas, surprisingly, the  $\delta$ -CR-EOMCC(2,3) results<sup>98</sup> of Ref. 90 are significantly lower for a reason that remains unclear to us. Note, however, that the CCSD excitation energies of Ref. 90 and ours (see Section 3.2) are in excellent agreement.

##### 3.1.2 BOD and BTD

Our results for 2,1,3-benzoxadiazole (BOD, also named benzofurazan in the literature) and 2,1,3-benzothiadiazole (BTD) are listed in Table 2. These building blocks are popular in many applications, e.g., they can be used as fluorescent probes for the former<sup>103</sup> and as an accepting moiety in solar cell materials for the latter.<sup>104</sup> Unsurprisingly, the ordering of the ESs is the same for the two compounds, the sulfur-bearing molecule presenting more redshifted values, except for the lowest triplet state. The lowest ES of BTD has a significant CT character,<sup>25</sup> whereas its BOD counterpart does not display significant separation between the electron and

Table 1: Vertical transition energies (in eV) of azulene. We provide the symmetry of all states as well as the nature of the transition. The rightmost columns list selected data from the literature.

State	6-31+G(d)		aug-cc-pVDZ		aug-cc-pVTZ		Lit.						
	CC3	CCSDT	CC3	CCSDT	CC3	CCSDT	Exp.	Exp.	Exp.	Th.	Th.	Th.	
$^1B_2$ (Val, $\pi \rightarrow \pi^*$ )	2.171	2.163	2.177		2.169		1.77 <sup>a</sup>	1.72 <sup>b</sup>	1.77 <sup>e</sup>	1.96 <sup>f</sup>	2.25 <sup>g</sup>	1.62 <sup>h</sup>	1.83 <sup>i</sup>
$^1A_1$ (CT, $\pi \rightarrow \pi^*$ )	3.959	3.965	3.878		3.843		3.57 <sup>a</sup>	3.56 <sup>c</sup>	3.56 <sup>e</sup>	3.81 <sup>f</sup>	3.99 <sup>g</sup>	3.41 <sup>h</sup>	3.46 <sup>i</sup>
$^1B_2$ (CT, $\pi \rightarrow \pi^*$ )	4.561	4.580	4.523		4.491			4.22 <sup>d</sup>	4.23 <sup>e</sup>	4.15 <sup>f</sup>	4.66 <sup>g</sup>	4.08 <sup>h</sup>	4.13 <sup>i</sup>
$^1A_2$ (Ryd.)	5.012	5.031	4.783		4.855			4.40 <sup>d</sup>	4.72 <sup>e</sup>		4.79 <sup>g</sup>		
$^1A_1$ (Val, $\pi \rightarrow \pi^*$ )	5.018	5.060	4.941		4.914				4.40 <sup>e</sup>	4.94 <sup>f</sup>	5.05 <sup>g</sup>	4.77 <sup>h</sup>	4.50 <sup>i</sup>
$^1B_1$ (Ryd.)	5.338	5.355	5.216		5.285				5.19 <sup>e</sup>		5.22 <sup>g</sup>		
$^3B_2$ (Val, $\pi \rightarrow \pi^*$ )	2.211		2.189				1.72 <sup>a</sup>						1.76 <sup>i</sup>
$^3A_1$ (Val, $\pi \rightarrow \pi^*$ )	2.430		2.466				2.38 <sup>a</sup>						2.26 <sup>i</sup>
$^3A_1$ (Val, $\pi \rightarrow \pi^*$ )	2.923		2.900				2.85 <sup>a</sup>						2.70 <sup>i</sup>
$^3B_2$ (Val, $\pi \rightarrow \pi^*$ )	4.203		4.161				3.86 <sup>a</sup>						3.87 <sup>i</sup>

<sup>a</sup>Photoelectron spectroscopy from Ref. 91; <sup>b</sup>0-0 energy in frozen matrix from Ref. 93; <sup>c</sup>0-0 energy from fluorescence study of Ref. 94; <sup>d</sup>0-0 energy from the fluorescence spectrum of the jet-cooled derivative in Ref. 95; <sup>e</sup>“Electronic energy” from pump-probe experiments of Ref. 96. Here, we simply assigned the two lowest Rydberg according to their energetic ordering; <sup>f</sup> CASPT2/6-31G(d) values from Ref. 87; <sup>g</sup>CCSDR(3)/DZ+P values from Ref. 88; <sup>h</sup> $\delta$ -CR-EOMCC(2,3)/cc-pVDZ values from Ref. 90; <sup>i</sup>DFT/MRCI values from Ref. 91, determined at the anionic geometry.

Table 2: Vertical transition energies (in eV) of BOD and BTB. See caption of Table 1 for more details.

2,1,3-benzoxadiazole (BOD)										
State	%T <sub>1</sub>	6-31+G(d)		aug-cc-pVDZ		aug-cc-pVTZ		Lit.		
		CC3	CCSDT	CC3	CCSDT	CC3	CCSDT	Exp.	Th.	
$^1B_2$ (Val, $\pi \rightarrow \pi^*$ )	88.6	4.706	4.794	4.575	4.661	4.520		4.00 <sup>a</sup>	4.16 <sup>b</sup>	
$^1A_1$ (Val, $\pi \rightarrow \pi^*$ )	83.5	4.989	4.990	4.940	4.945	4.906		4.40 <sup>a</sup>	4.85 <sup>b</sup>	
$^1A_2$ (Val, $n \rightarrow \pi^*$ )	86.9	5.461	5.483	5.368	5.396	5.284				
$^1B_1$ (Val, $n/\sigma \rightarrow \pi^*$ )	85.6	5.997	6.009	5.899	5.915	5.833				
$^3B_2$ (Val, $\pi \rightarrow \pi^*$ )	97.5	2.763		2.751		2.739				
$^3A_1$ (Val, $\pi \rightarrow \pi^*$ )	97.2	4.181		4.118		4.084				

2,1,3-benzothiadiazole (BTB)										
State	%T <sub>1</sub>	6-31+G(d)		aug-cc-pVDZ		aug-cc-pVTZ		Lit.		
		CC3	CCSDT	CC3	CCSDT	CC3	CCSDT	Exp.	Th.	
$^1B_2$ (CT, $\pi \rightarrow \pi^*$ )	86.1	4.419	4.481	4.301	4.363	4.229		3.77 <sup>a</sup>	3.94 <sup>b</sup>	
$^1A_1$ (Val, $\pi \rightarrow \pi^*$ )	86.5	4.465	4.477	4.405	4.417	4.359		4.05 <sup>a</sup>	4.11 <sup>b</sup>	
$^1A_2$ (Val, $n \rightarrow \pi^*$ )	87.7	4.977	4.984	4.886	4.897	4.795				
$^1B_1$ (Val, $n/\sigma \rightarrow \pi^*$ )	86.1	5.616	5.620	5.520	5.525	5.417				
$^3B_2$ (Val, $\pi \rightarrow \pi^*$ )	97.3	2.833		2.836		2.820		2.28 <sup>c</sup>		
$^3A_1$ (Val, $\pi \rightarrow \pi^*$ )	97.3	3.646		3.551		3.485				

<sup>a</sup>Vapor phase 0-0 energies from Ref. 99; <sup>b</sup>ADC(3)/aug-cc-pVDZ value from Ref. 100; for the lowest singlet of BTB, a value of 4.28 eV was reported as basis set extrapolated TBE in Ref. 25 whereas a 4.15 eV TD-DFT estimate is given in Ref. 101; <sup>c</sup>0-0 phosphorescence measured in a frozen dichlorobenzene matrix from Ref. 102. The same work reports a 0-0 energy of 3.52 eV for the lowest singlet, significantly redshifted as compared to the vapor measurement of Ref. 99.

the hole according to popular metrics.<sup>64–66</sup> As can be seen in Table 2, rather usual basis set effects are obtained with regular decrease of the transition energies as the basis set size increases, although the amplitude of the changes are strongly state-dependent, as illustrated by the “insensitivity” to basis set effect of the lowest triplet state. For the two lowest triplet ESs of  $\pi \rightarrow \pi^*$  nature, very large  $\%T_1$  ( $> 97\%$ ) are calculated, and one can be confident that the CC3 values are accurate. For the singlet ESs, the differences between the CC3 and CCSDT results are of the order of 0.02 eV, except for the lowest  $^1B_2$  ES: the CC3 estimates (4.71 and 4.42 eV for BOD and BTD, respectively) are significantly smaller than their CCSDT counterparts (4.79 and 4.48 eV, respectively). Such trend is typical of CT states,<sup>25,105</sup> and seems to apply to the first ES of BOD though the tested metrics did not revealed a significant CT character.

For substituted furazans, several TD-DFT studies can be found,<sup>106–108</sup> but apparently the only previous investigation of the building block itself is the work of Prlj *et al.*<sup>100</sup> who studied the  $L_a/L_b$  (or  $^1B_2/^1A_1$ ) ordering in several bicyclic systems. This work reports CC2 transition energies closely matching the present values (4.588 and 4.887 eV), whereas the ADC(3) VTEs show a larger gap between the two ESs (see rightmost column in Table 2). The vapour spectrum of BOD was measured in 1969,<sup>99</sup> and the experimental 0-0 energies are shifted by approximately  $-0.5$  eV compared to our VTEs, which is a typical trend. For BTD, more measurements are available<sup>99,102,109,110</sup> and the lowest transitions were treated previously with TD-DFT<sup>100,101,111,112</sup> and wave function approaches,<sup>25,100</sup> a few relevant values being summarized in Table 2. The gap between the two lowest singlet transitions is around 0.10 eV according to our data, the  $^1B_2$  ES being the lowest-energy state. Previous CC2 and ADC(3) values report a similar pattern.<sup>100</sup> In contrast CCSD/*aug-cc-pVTZ* yields almost degenerated transitions but with the incorrect ordering (see the SI). The experimental BTD 0-0 energies of Ref. 99 are red-shifted by  $-0.23$  and  $-0.35$  eV as compared to those of BOD for the  $^1B_2$  and  $^1A_1$  transitions, respectively. The CC3/*aug-cc-pVTZ* heteroatomic shifts of the vertical energies are of the same order of magnitude, i.e.,  $-0.29$  and  $-0.55$  eV.

### 3.1.3 DPP

Due to its intense absorption around 500 nm, DPP is also an extraordinary popular moiety to design dyes used in automotive paints, light harvesting applications, or fluorescent sensors.<sup>113</sup> While there exist many TD-DFT calculations of DPP-containing compounds in the literature, we could not find previous theoretical works devoted to the chromogen itself, but for a 2009 TD-DFT contribution,<sup>114</sup> and studies limited to the solvation effects of the lowest transition.<sup>111,112</sup> According to our calculations (Table 3) the lowest singlet ES is a bright  $^1B_u$  that interestingly lies more than 1.5 eV above the corresponding triplet, hinting at small intersystem crossing. Next, one finds two (nearly) dark ESs of  $^1A_u$  ( $n \rightarrow \pi^*$ ) and  $^1A_g$  ( $\pi \rightarrow \pi^*$ ) symmetries, whereas the fourth ESs is a dark  $^1B_g$  ( $\pi \rightarrow \pi^*$ ). For all eight transitions listed in Table 3, the basis set effects are rather small, with variations of ca.  $-0.05$  to  $-0.10$  eV between the 6-31+G(d) and *aug-cc-pVTZ* VTEs. With the former basis set, we could perform

CCSDT calculations, and the outcome hints that the CC3 VTEs are slightly too low by approximately 0.03-0.04 eV for the four singlet ESs. As in BOD and BTD, very large  $\%T_1$  are found for the triplet ESs, and one can likely view the CC3/*aug-cc-pVTZ* excitation energies as reliable TBEs for the triplets.

### 3.1.4 FF, PP, and TT

Furo[3,2-*b*]furan (FF), 1,4-dihydropyrrolo[3,2-*b*]pyrrole (PP) and thieno[3,2-*b*]thiophene (TT) are centrosymmetric bicyclic molecules encompassing two identical and fused five member cycles. TT is often used as a linker in  $\pi$ -delocalized polymers,<sup>115</sup> whereas PP is an increasingly popular accepting moiety, notably in quadrupolar systems showing large nonlinear optical responses.<sup>116</sup> Our results are collected in Table 4.

According to our calculations, the lowest singlet ES of FF is of Rydberg character. It presents almost the same VTE as the bright  $^1B_u$ , the latter being typical in  $\pi$ -delocalized dyes of  $C_{2h}$  symmetry. The hallmark dark  $\pi \rightarrow \pi^*$   $^1A_g$  ES lies approximately 0.6 eV higher. As expected it has a smaller single excitation character ( $\%T_1 = 82.6\%$ ) than the other ESs treated here, but the difference between the CC3 and CCSDT VTEs remains small ( $-0.02$  eV). This can be compared to the  $^1A_g$  ES in hexatriene ( $\%T_1 = 65.3\%$ ) for which the CC3-CCSDT difference is about five times larger.<sup>29</sup> We have also found two other Rydberg transitions of  $B_g$  symmetry, and two  $\pi \rightarrow \pi^*$  triplet ESs with very large  $\%T_1$ , strongly redshifted compared to the corresponding singlet excitations. Going from *aug-cc-pVDZ* to *aug-cc-pVTZ* induces an increase/decrease of the VTEs for the Rydberg/valence transitions. In PP, the CC3/*aug-cc-pVTZ* calculations indicate that the four lowest singlet transitions are of Rydberg nature (the  $\pi \rightarrow \pi^*$   $^1B_u$  lies higher, at 5.499 eV according to CC3/*aug-cc-pVTZ*). All these four ESs have a strong single-excitation character. In contrast, in the triplet manifold, the lowest-energy ES has a valence character, the two following ones being of Rydberg nature. The picture is vastly different in TT, in which one first notices two low-lying nearly-degenerated singlet valence ESs of  $B_u$  symmetry (see also the discussion below), the Rydberg transitions appearing at slightly higher energy. In the triplet manifold of TT, three valence  $\pi \rightarrow \pi^*$  ESs could be identified. All seven ESs of TT listed in Table 4 are characterized by  $\%T_1 > 85\%$ , highly similar CC3 and CCSDT VTEs, and rather mild basis set effects.

For FF, we have found only one previous study,<sup>117</sup> that reported an ADC(2) value for the lowest  $^1B_u$  transition in reasonable agreement with the present estimate. For the non-substituted PP we could not find previous theoretical nor experimental works. In contrast, TT has been studied using various levels of theory.<sup>111,112,117</sup> For its two lowest ESs, a refined theoretical study proposed by the Corminboeuf group,<sup>117</sup> highlighted the challenge of obtaining an accurate ordering with TD-DFT (almost) independently of the selected exchange-correlation functional. At the CCSD/*aug-cc-pVTZ* level, these two ESs are quite strongly mixed in terms of underlying MOs (see Table S10 in the SI). Our best estimates actually provide the same ordering as the CC2 and SAC-CI approaches used in Ref. 117, i.e., the lowest ES is dominated by a HOMO  $-1$  to LUMO character, whereas the second ES

Table 3: Vertical transition energies (in eV) of DPP. See caption of Table 1 for more details.

State	%T <sub>1</sub>	6-31+G(d)		aug-cc-pVDZ		aug-cc-pVTZ	Lit. Th.
		CC3	CCSDT	CC3	CCSDT	CC3	
<sup>1</sup> B <sub>u</sub> (Val, π → π*)	88.4	3.650	3.683	3.541		3.535	3.42 <sup>a</sup>
<sup>1</sup> A <sub>u</sub> (Val, n → π*)	83.7	3.953	3.989	3.907		3.863	3.75 <sup>a</sup>
<sup>1</sup> A <sub>g</sub> (Val, π → π*)	87.0	3.959	4.009	3.872		3.910	3.95 <sup>a</sup>
<sup>1</sup> B <sub>g</sub> (Val, n → π*)	81.5	4.397	4.426	4.324		4.309	4.21 <sup>a</sup>
<sup>3</sup> B <sub>u</sub> (Val, π → π*)	97.4	1.957		1.923		1.927	
<sup>3</sup> A <sub>g</sub> (Val, π → π*)	97.3	3.804		3.751		3.743	
<sup>3</sup> A <sub>u</sub> (Val, n → π*)	94.9	3.867		3.787		3.781	
<sup>3</sup> B <sub>g</sub> (Val, n → π*)	94.5	4.310		4.240		4.226	

<sup>a</sup>TD-PBE0/6-311++G(d,p) from Ref. 114.

Table 4: Vertical transition energies (in eV) of FF, PP, and TT. See caption of Table 1 for more details.

Furo[3,2- <i>b</i> ]furan (FF)							
State	%T <sub>1</sub>	6-31+G(d)		aug-cc-pVDZ		aug-cc-pVTZ	Lit. Th.
		CC3	CCSDT	CC3	CCSDT	CC3	
<sup>1</sup> A <sub>u</sub> (Ryd)	93.4	5.590	5.602	5.357	5.361	5.430	5.63 <sup>a</sup>
<sup>1</sup> B <sub>u</sub> (Val, π → π*)	91.5	5.644	5.672	5.500	5.526	5.463	
<sup>1</sup> B <sub>g</sub> (Ryd)	93.4	5.985	6.002	5.783	5.789	5.859	
<sup>1</sup> B <sub>g</sub> (Ryd)	93.1	6.148	6.165	5.934	5.942	5.993	
<sup>1</sup> A <sub>g</sub> (Val, π → π*)	82.6	6.250	6.228	6.080	6.067	6.040	
<sup>3</sup> B <sub>u</sub> (Val, π → π*)	97.9	3.661		3.601		3.578	
<sup>3</sup> A <sub>g</sub> (Val, π → π*)	98.2	4.956		4.897		4.869	
1,4-Dihydropyrrolo[3,2- <i>b</i> ]pyrrole (PP)							
State	%T <sub>1</sub>	6-31+G(d)		aug-cc-pVDZ		aug-cc-pVTZ	Lit. Th.
		CC3	CCSDT	CC3	CCSDT	CC3	
<sup>1</sup> A <sub>u</sub> (Ryd)	92.8	4.558	4.563	4.454	4.445	4.545	
<sup>1</sup> B <sub>g</sub> (Ryd)	92.5	4.761	4.768	4.656	4.649	4.746	
<sup>1</sup> A <sub>u</sub> (Ryd)	92.0	5.088	5.078	5.020	4.994	5.133	
<sup>1</sup> B <sub>g</sub> (Ryd)	93.1	5.275	5.281	5.067	5.055	5.145	
<sup>3</sup> B <sub>u</sub> (Val, π → π*)	97.9	3.921		3.867		3.841	
<sup>3</sup> A <sub>u</sub> (Ryd)	97.4	4.529		4.431		4.524	
<sup>3</sup> B <sub>g</sub> (Ryd)	97.3	4.739		4.641		4.733	
Thieno[3,2- <i>b</i> ]thiophene (TT)							
State	%T <sub>1</sub>	6-31+G(d)		aug-cc-pVDZ		aug-cc-pVTZ	Lit. Th.
		CC3	CCSDT	CC3	CCSDT	CC3	
<sup>1</sup> B <sub>u</sub> (Val, π → π*)	87.5	5.100	5.096	5.003	5.004	4.964	5.04 <sup>b</sup>
<sup>1</sup> B <sub>u</sub> (Val, π → π*)	90.6	5.439	5.460	5.301	5.320	5.224	5.29 <sup>b</sup>
<sup>1</sup> B <sub>g</sub> (Ryd)	90.3	5.465	5.465	5.455	5.454	5.412	
<sup>1</sup> A <sub>u</sub> (Ryd)	91.6	5.487	5.485	5.483	5.474	5.518	
<sup>3</sup> B <sub>u</sub> (Val, π → π*)	97.7	3.488		3.490		3.465	
<sup>3</sup> B <sub>u</sub> (Val, π → π*)	97.2	4.376		4.301		4.261	
<sup>3</sup> A <sub>g</sub> (Val, π → π*)	97.9	4.669		4.613		4.580	

<sup>a</sup>ADC(2)/cc-pVQZ value from Ref. 117; <sup>b</sup>SAC-CI/cc-pVTZ value from Ref. 117.

is mainly corresponding to a HOMO to LUMO excitation.

### 3.1.5 Phthalazine and quinoxaline

We also consider two diazanaphthalenes having to  $C_{2v}$  point group symmetry that are popular building blocks in dye chemistry, namely phthalazine and quinoxaline.<sup>118,119</sup> The latter presents lowest singlet and triplet ESs of different chemical natures, making quinoxaline derivatives particularly appealing for purely organic TADF applications, thanks to an exceptionally efficient intersystem crossing.<sup>120</sup> We report in Table 5 numerous singlet and a few triplet excited states for these two compounds.

The impact of including full (CCSDT) rather than approximate (CC3) triples is never large yet appears not insignificant for several ESs of phthalazine with increase of the VTEs by 0.04 eV for the two highest ESs considered in Table 5 as well as for the lowest singlet state of  $B_2$  symmetry. For quinoxaline, the largest differences between the CCSDT/6-31+G(d) and CC3/6-31+G(d) transition energies are found for two CT transitions:  $^1B_2$  (+0.06 eV) and  $^1B_1$  (+0.07 eV). As already explained, such slight CC3 underestimation of the CT VTEs has been reported before.<sup>25,105</sup> Regarding basis set effects, nothing beyond expectations emerges with a mean decrease of -0.04 eV when switching from *aug-cc-pVDZ* to *aug-cc-pVTZ* for quinoxaline, the actual shift being not very ES-dependent (the corrections go from -0.015 to -0.057 eV). The scenario is similar for phthalazine CT and valence excitations (mean impact of going from *aug-cc-pVDZ* to *aug-cc-pVTZ* is -0.03 eV, with values ranging from -0.001 to -0.060 eV), but both the sign and magnitude of the basis corrections are vastly different for the two Rydberg transitions.

Several theoretical and experimental transition energies have been previously given for both systems,<sup>121-126</sup> though, to the best of our knowledge, none reported so many ESs, nor considered third-order CC models. We can thus consider the VTEs of Table 5 as the (most accurate published to date. When comparing to experimental data, it appears that, as for the above-discussed compounds, the VTEs exceed the energies of the experimental peaks<sup>121</sup> typically by 0.2-0.4 eV, whereas even larger differences are found with respect to the measured 0-0 energies.<sup>123</sup> The six CASPT2/cc-pVQZ values of Ref. 124 are in reasonable agreement with the present CC3/*aug-cc-pVTZ* results with a mean absolute deviation (MAD) of 0.25 eV, the usual CASPT2 trend of yielding too small VTEs being clearly highlighted here, except for the first  $^1B_2$  transition in phthalazine. The deviations with respect to the CC2/*aug-cc-pVDZ* data of Ref. 125 are small (MAD of 0.09 eV) if one excludes the  $^3A_1$  transition of quinoxaline for which a very large difference of 0.89 eV is found between the present value and the literature estimate. Given that the % $T_1$  value associated with this state is very large (96.9%) and that our CC2/*aug-cc-pVTZ* result computed on the geometry used in the present study is only 0.16 eV off its CC3 counterpart, this large difference is somewhat surprising.

### 3.1.6 TTF

Tetrathiafulvalene (TTF) possesses very specific redox properties,<sup>127,128</sup> but its optical signatures are also of interest, notably due to its accepting properties in CT complexes<sup>127</sup> as well as to the presence of several low-lying  $\pi \rightarrow \sigma^*$  tran-

sitions, that are rather unusual in organic derivatives.<sup>129</sup> We consider here the closed-shell singlet form of TTF (Table 6), and determine VTEs for 8 singlet and 6 triplet ESs. It is noteworthy that we enforce planarity during the optimization, to benefit from the high  $D_{2h}$  symmetry, whereas the actual structure is very slightly bent.<sup>130</sup>

The basis set effects seem under control for TTF. We observe, in particular, limited changes between the *aug-cc-pVDZ* and *aug-cc-pVTZ* data, with an average downshift of -0.03 eV (MAD: 0.05 eV), and a maximal change of -0.09 eV ( $^1B_{1u}$ ). The two Rydberg ESs are the only ones for which going from the double- to the triple- $\zeta$  basis set actually increases the computed transition energy, a common pattern for the present set of molecules. It is also noteworthy that for all transitions, the differences between the CCSDT and CC3 transitions, as given with the 6-31+G(d) basis set, are small, none of them exceeding 0.03 eV, consistent with the fact that all % $T_1$  are rather large. All these elements give us confidence that the reported VTEs are accurate.

Interestingly, previous TD-DFT,<sup>134,135</sup> CC2,<sup>135</sup> and CASPT2<sup>129,135</sup> investigations are available for TTF. If one disregards the Rydberg transitions, the ordering of the CASPT2 ESs reported in 2002<sup>129</sup> matches the present CC3 one, but these “old” CASPT2 VTEs are notably too low, with underestimations of roughly -0.4 eV or more for most states. The more recent CASPT2 energies are closer to our present values, yet remain too small. In contrast the TD-DFT calculations performed with the B3P86 global hybrid,<sup>134</sup> as well as CC2 calculations<sup>135</sup> provide estimates closer to the current results. The UV/Vis spectra of TTF have been measured by several groups in apolar solvents,<sup>131-133</sup> allowing comparisons for three transitions. As expected in such VTE *versus*  $\lambda_{\max}$  comparison, the CC3 values are larger by 0.1-0.6 eV, which indicates that the data of Table 6 are reasonable.

## 3.2 Benchmarks

To define our TBEs, we typically consider: (i) CCSDT/double- $\zeta$  [6-31+G(d), or *aug-cc-pVDZ*] VTEs corrected for basis set effects thanks to the difference between CC3/double- $\zeta$  and CC3/*aug-cc-pVTZ* for singlet ESs, and (ii) select the CC3/*aug-cc-pVTZ* VTEs for triplet ESs. The complete list of TBEs and each specific protocol employed to obtain these are available in Table S11 in the SI.

CC3 nor CCSDT are exact theories, so before assessing other methods, let us briefly discuss the expected accuracy of the present TBEs. For the singlet ESs, our reference values are essentially of CCSDT quality and none of the ES treated here has a significant double-excitation character. More specifically, all % $T_1$  (that could be obtained) exceed 80%, and the variations between CC3 and CCSDT are typically very small. While this provides confidence that the TBEs are accurate, they are likely not precise enough to fairly compare methods that yield highly similar results and are closely related, e.g., CCSDR(3) and CCSD(T)(a)\*. For the triplet ESs, our reference values, of CC3/*aug-cc-pVTZ* quality, are likely sufficient to assess the tested methods. They are three reasons for this assertion. First, all triplet ESs treated here have very large % $T_1$ . Second, in the full QUEST database, the mean absolute error obtained with CC3/*aug-cc-*

Table 5: Vertical transition energies (in eV) of phthalazine and quinoxaline. See caption of Table 1 for more details.

Phthalazine									
State	6-31+G(d)		<i>aug-cc-pVDZ</i>		<i>aug-cc-pVTZ</i>		Lit.		
	CC3	CCSDT	CC3	CC3	Exp.	Exp.	Th.	Th.	Th.
<sup>1</sup> A <sub>2</sub> (CT, $n \rightarrow \pi^*$ )	3.986	4.012	3.889	3.872	3.61 <sup>a</sup>	3.01 <sup>c</sup>	3.68 <sup>d</sup>	3.74 <sup>e</sup>	
<sup>1</sup> B <sub>1</sub> (CT, $n \rightarrow \pi^*$ )	4.427	4.446	4.317	4.283	3.92 <sup>a</sup>	3.72 <sup>c</sup>	4.12 <sup>d</sup>	4.20 <sup>e</sup>	
<sup>1</sup> A <sub>1</sub> (Val, $\pi \rightarrow \pi^*$ )	4.539	4.517	4.501	4.473	4.13 <sup>a</sup>	4.09 <sup>c</sup>		4.46 <sup>e</sup>	
<sup>1</sup> B <sub>2</sub> (Val, $\pi \rightarrow \pi^*$ )	5.364	5.406	5.201	5.146	4.86 <sup>a</sup>	4.59 <sup>c</sup>	5.27 <sup>d</sup>	4.98 <sup>e</sup>	
<sup>1</sup> B <sub>1</sub> (CT, $n \rightarrow \pi^*$ )	5.662	5.690	5.561	5.520					
<sup>1</sup> A <sub>2</sub> (Mixed)	5.954	6.052	5.745	5.744					
<sup>1</sup> A <sub>2</sub> (CT, $n \rightarrow \pi^*$ )	6.037	6.043	5.930	5.870		5.33 <sup>c</sup>			
<sup>1</sup> A <sub>1</sub> (Val, $\pi \rightarrow \pi^*$ )	6.243	6.204	6.185	6.148					
<sup>1</sup> A <sub>2</sub> (Ryd)	6.606	6.620	6.362	6.430					
<sup>1</sup> B <sub>2</sub> (Ryd)	6.379	6.408	6.133	6.234					
<sup>1</sup> A <sub>1</sub> (Val, $\pi \rightarrow \pi^*$ )	6.510	6.554	6.410	6.364	5.84 <sup>a</sup>				
<sup>3</sup> B <sub>2</sub> (Val, $\pi \rightarrow \pi^*$ )	3.452		3.440	3.430	2.85 <sup>b</sup>	2.74 <sup>c</sup>		3.42 <sup>e</sup>	
<sup>3</sup> A <sub>2</sub> (CT, $n \rightarrow \pi^*$ )	3.721		3.628	3.626				3.48 <sup>e</sup>	
<sup>3</sup> B <sub>1</sub> (CT, $n \rightarrow \pi^*$ )	3.801		3.720	3.711				3.67 <sup>e</sup>	
<sup>3</sup> A <sub>1</sub> (Val, $\pi \rightarrow \pi^*$ )	4.333		4.266	4.224				4.30 <sup>e</sup>	

Quinoxaline									
State	6-31+G(d)		<i>aug-cc-pVDZ</i>		<i>aug-cc-pVTZ</i>		Lit.		
	CC3	CCSDT	CC3	CC3	Exp.	Exp.	Exp.	Th.	Th.
<sup>1</sup> B <sub>1</sub> (Val, $n \rightarrow \pi^*$ )	3.944	3.954	3.831	3.790	3.58 <sup>a</sup>	3.36 <sup>c</sup>	3.36 <sup>f</sup>	3.83 <sup>d</sup>	3.76 <sup>e</sup>
<sup>1</sup> A <sub>1</sub> (Val, $\pi \rightarrow \pi^*$ )	4.333	4.318	4.295	4.263	4.00 <sup>a</sup>	3.97 <sup>c</sup>	3.96 <sup>f</sup>		4.26 <sup>e</sup>
<sup>1</sup> B <sub>2</sub> (CT, $\pi \rightarrow \pi^*$ )	4.772	4.827	4.643	4.586	4.34 <sup>a</sup>	4.09 <sup>c</sup>		4.89 <sup>d</sup>	4.45 <sup>e</sup>
<sup>1</sup> A <sub>2</sub> (Val, $n \rightarrow \pi^*$ )	5.220	5.233	5.109	5.087				5.39 <sup>d</sup>	5.03 <sup>e</sup>
<sup>1</sup> A <sub>2</sub> (Val, $n \rightarrow \pi^*$ )	5.549	5.547	5.442	5.390					
<sup>1</sup> A <sub>1</sub> (CT, $\pi \rightarrow \pi^*$ )	5.770	5.761	5.716	5.674	5.35 <sup>a</sup>	5.33 <sup>c</sup>	5.36 <sup>f</sup>		
<sup>1</sup> B <sub>1</sub> (CT, $n \rightarrow \pi^*$ )	6.368	6.433	6.163	6.140		5.70 <sup>c</sup>			
<sup>1</sup> B <sub>2</sub> (Val, $\pi \rightarrow \pi^*$ )	6.489	6.511	6.332	6.277					
<sup>3</sup> B <sub>2</sub> (Val, $\pi \rightarrow \pi^*$ )	3.286		3.270	3.255		2.68 <sup>c</sup>			3.26 <sup>e</sup>
<sup>3</sup> B <sub>1</sub> (Val, $n \rightarrow \pi^*$ )	3.461		3.368	3.352		3.04 <sup>c</sup>			3.31 <sup>e</sup>
<sup>3</sup> A <sub>1</sub> (Val, $\pi \rightarrow \pi^*$ )	4.012		3.919	3.875					4.76 <sup>e</sup>

<sup>a</sup>MCD spectra measured in *n*-heptane from Ref. 121; <sup>b</sup>0-0 phosphorescence in a frozen matrix from Ref. 122; <sup>c</sup>0-0 energy collected in Ref. 123 (see references therein); <sup>d</sup>CASPT2/*cc-pVQZ* values from Ref. 124; <sup>e</sup>CC2/*aug-cc-pVDZ* data from Ref. 125; <sup>f</sup> Gas-Phase 0-0 energies from Ref. 126

Table 6: Vertical transition energies (in eV) of TTF. See caption of Table 1 for more details.

TTF									
State	%T <sub>1</sub>	6-31+G(d)		<i>aug-cc-pVDZ</i>		<i>aug-cc-pVTZ</i>		Litt.	
		CC3	CCSDT	CC3	CC3	Exp.	Th.	Th.	Th.
<sup>1</sup> B <sub>3u</sub> (Val, $\pi \rightarrow \sigma^*$ )	90.1	2.958	2.971	2.866	2.787	2.72 <sup>a</sup>	2.08 <sup>b</sup>	2.57 <sup>c</sup>	2.68 <sup>d</sup> 2.42 <sup>e</sup>
<sup>1</sup> B <sub>2u</sub> (Val, $\pi \rightarrow \pi^*$ )	87.9	4.159	4.190	3.795	3.742	3.35 <sup>a</sup>	3.05 <sup>b</sup>	3.30 <sup>c</sup>	3.46 <sup>d</sup> 3.31 <sup>e</sup>
<sup>1</sup> B <sub>1g</sub> (Val, $\pi \rightarrow \sigma^*$ )	90.5	4.059	4.067	4.013	3.979		3.31 <sup>b</sup>	3.72 <sup>c</sup>	
<sup>1</sup> B <sub>2g</sub> (Val, $\pi \rightarrow \sigma^*$ )	89.3	4.083	4.082	4.057	4.048		3.41 <sup>b</sup>	3.92 <sup>c</sup>	
<sup>1</sup> B <sub>3u</sub> (Ryd.)	92.8	4.192	4.193	4.048	4.113		3.63 <sup>b</sup>	4.25 <sup>c</sup>	
<sup>1</sup> B <sub>3g</sub> (Val, $\pi \rightarrow \pi^*$ )	86.2	4.496	4.521	4.264	4.218		3.44 <sup>b</sup>	3.72 <sup>c</sup>	
<sup>1</sup> B <sub>1u</sub> (Val, $\pi \rightarrow \pi^*$ )	90.6	4.805	4.816	4.601	4.514	3.91 <sup>a</sup>	4.01 <sup>b</sup>	4.28 <sup>c</sup>	4.25 <sup>d</sup> 4.18 <sup>e</sup>
<sup>1</sup> B <sub>2g</sub> (Ryd.)	92.0	4.648	4.649	4.495	4.551		3.80 <sup>b</sup>		
<sup>3</sup> B <sub>3u</sub> (Val, $\pi \rightarrow \sigma^*$ )	96.7	2.804		2.727	2.652		1.92 <sup>b</sup>	2.33 <sup>c</sup>	
<sup>3</sup> B <sub>1u</sub> (Val, $\pi \rightarrow \pi^*$ )	97.7	3.158		3.055	2.993		2.76 <sup>b</sup>	2.64 <sup>c</sup>	
<sup>3</sup> B <sub>2u</sub> (Val, $\pi \rightarrow \pi^*$ )	97.1	3.383		3.160	3.123		2.89 <sup>b</sup>	2.64 <sup>c</sup>	
<sup>3</sup> B <sub>3g</sub> (Val, $\pi \rightarrow \pi^*$ )	97.4	3.565		3.431	3.400		3.11 <sup>b</sup>	2.90 <sup>c</sup>	
<sup>3</sup> B <sub>1g</sub> (Val, $\pi \rightarrow \sigma^*$ )	96.8	3.862		3.833	3.803				
<sup>3</sup> B <sub>2g</sub> (Val, $\pi \rightarrow \sigma^*$ )	96.8	3.946		3.942	3.916				

<sup>a</sup> $\lambda_{\max}$  in hexane from Ref. 131; very similar values have been reported in other measurements; <sup>b</sup>MS-CASPT2 values from Ref. 129; <sup>c</sup>TD-DFT (B3P86/*aug-cc-pVDZ*) values from Ref. 134; <sup>d</sup>CC2/*aug-TZVPP* values from Ref. 135; <sup>e</sup> $\pi$ -CASPT2C/aV(T+d)Z values from Ref. 135;



pVTZ (as compared to higher levels of theory) is as small as 0.01 eV.<sup>29</sup> Third, the three other CC methods including corrections for the triples, namely, CCSDR(3), CCSD(T)(a)\*, and CCSDT-3, have not been implemented for triplet ESs, so that only methods significantly less advanced than CC3 are benchmarked below.

In Table 7, we report the statistical results obtained considering the full set of data (only singlets are included for all CC methods including triples): mean signed error (MSE), mean absolute error (MAE), root mean square error (RMSE) and the standard deviation of the errors (SDE). For the present set of excitations, the distribution of the errors in VTEs (with respect to the TBEs/aug-cc-pVTZ) is represented in Figure 2.

On the left-hand-side of Table 7, one can find the statistical results obtained considering all ESs. EOM-MP2 appears to strongly overestimate the VTEs and exhibits a large dispersion. In short, it cannot be recommended for the present bicyclic compounds. Amongst the computationally light models, CIS(D) is clearly a better option though the associated MAE remains quite large, 0.24 eV, a rather typical error bar for this level of theory.<sup>21,23,29,136,137</sup> EOM-MP2 and CIS(D) performances are clearly inferior to the ones of two other popular models, namely ADC(2) and CC2 that both deliver very reasonable estimates of the VTEs for the present molecular set, especially ADC(2) that enjoys a trifling MSE and a MAE as small as 0.10 eV. For both CC2 and ADC(2), these trends are compatible with the conclusions obtained from the QUEST database,<sup>29</sup> as well as in many previous works benchmarking ADC(2) and/or CC2 for optical properties.<sup>21,23,26,28,81,137-141</sup> For CC2, the two spin-scaled approaches (SOS and SCS) significantly deteriorate the CC2 MSE and MAE, leading to a clear overestimation. However, both SOS-CC2 and SCS-CC2 do decrease CC2’s dispersion, especially SCS-CC2 that returns a SDE of 0.09 eV only, a level of consistency that can only be further improved with higher-level approaches according to the data of Table 7. Such accuracy drop and gain in consistency of the spin-scaled CC2 methods has been reported before.<sup>24,136,137,142</sup> For ADC(2), none of the two tested SOS parameters is beneficial as compared to the original method, but it is very clear that the default Q-CHEM parametrization<sup>85</sup> is superior to its TURBOMOLE analog for the present set. It also appears that STEOM-CCSD is a valuable approach with small MSE, MAE, and SDE. However, as explained in the computational details, several ESs that are challenging have been removed from the STEOM-CCSD evaluation set, making the statistical quantities possibly biased. Nevertheless, the similarity between the STEOM-CCSD and CC2 performances observed in the present study was already underlined in earlier studies.<sup>21,23,24,75</sup>

Moving now to methods with higher  $O(N^6)$  scaling, one notices that CCSD yields too large VTEs and a SDE comparable to the CC2 one. The overestimation trend of CCSD was again reported by various groups, though with magnitudes depending significantly on the actual test set,<sup>26,29,75,141,143-145</sup> an aspect discussed below. In contrast, ADC(3) delivers too small transition energies (MSE of  $-0.10$  eV) and a rather large dispersion (SDE of 0.22 eV). This relatively poor perfor-

mance of ADC(3) is consistent with our findings for smaller compounds,<sup>45</sup> but can be efficiently mitigated by averaging with the ADC(2) VTEs. Indeed, the error patterns of ADC(2) and ADC(3) are opposite,<sup>21</sup> and the simple average between the results of these two methods is effective: ADC(2.5), which has in practice the same computational cost as ADC(3), is the only  $O(N^6)$  method delivering MSE, MAE, RMSE, and SDE all smaller than 0.10 eV for the present set.

To finish, we have assessed four CC methods including triples against the CCSDT-quality reference data for the singlet transitions. The two perturbative approaches, CCSD(T)(a)\* and CCSDR(3), deliver very similar statistical errors and can be essentially viewed as equivalent for practical purposes. Such similarity was reported by Matthews and Watson for very compact compounds,<sup>76</sup> but with significantly smaller deviations as compared to CCSDT. Turning to the two CC approaches with approximated iterative triples, namely CCSDT-3 and CC3, the latter seems to have the edge for the present set, with average errors below the chemical accuracy threshold (0.043 eV). We note that a similar ranking was reported in 2017 for small molecules.<sup>141</sup>

The central section of Table 7 reports MAEs obtained for various subsets. We underline that the CT and  $\pi \rightarrow \sigma^*$  subsets are both limited in size (13 and 6 ESs) and nature (rather weak CT and transitions found in TTF only, respectively). Hence, the present trends should be analyzed cautiously. Most tested approaches deliver rather similar MAEs for the singlet and triplet ESs. However, CCSD is clearly more accurate for the triplets, in line with their larger  $\%T_1$  values than the singlets, whereas both STEOM-CCSD and CIS(D) apparently show the opposite behavior with better performances for the singlets. Surprisingly, most methods provide more accurate Rydberg VTEs than valence VTEs; the differences are especially large for CIS(D), CCSD, ADC(3), ADC(2.5) and all CC models including triples with significantly smaller MAEs for the Rydberg transitions. Although such trend are not unprecedented,<sup>29</sup> the differences between valence and Rydberg MAEs are quite large here. Interestingly, for much small systems, Kannar, Tajti, and Szalay reported that CC2 was much less accurate for the Rydberg transitions,<sup>141</sup> an effect that we do not observe here. We believe that this might be related to the low-lying nature of the transitions considered here whereas the Rydberg transitions of Ref. 141 correspond to high-energy ESs with a very diffuse character. For the present set of ESs, one also notices significant differences of MAEs for the  $n \rightarrow \pi^*$  and  $\pi \rightarrow \pi^*$  transitions, the latter being typically more accurately treated, except with STEOM-CCSD.

Let us now turn towards the impact of the molecular size, so as to investigate if larger compounds are more or less challenging than smaller ones for the different methods. In the three rightmost columns of Table 7, we compare the MAEs determined for the present set to those reported in the QUEST database for molecules containing 1–3 and 4–6 non-hydrogen atoms.<sup>29</sup> One can broadly divide the various methods in three groups. In the first group, one notices a significant deterioration of the performance as the system size increases, hinting that the method cannot be reasonably rec-

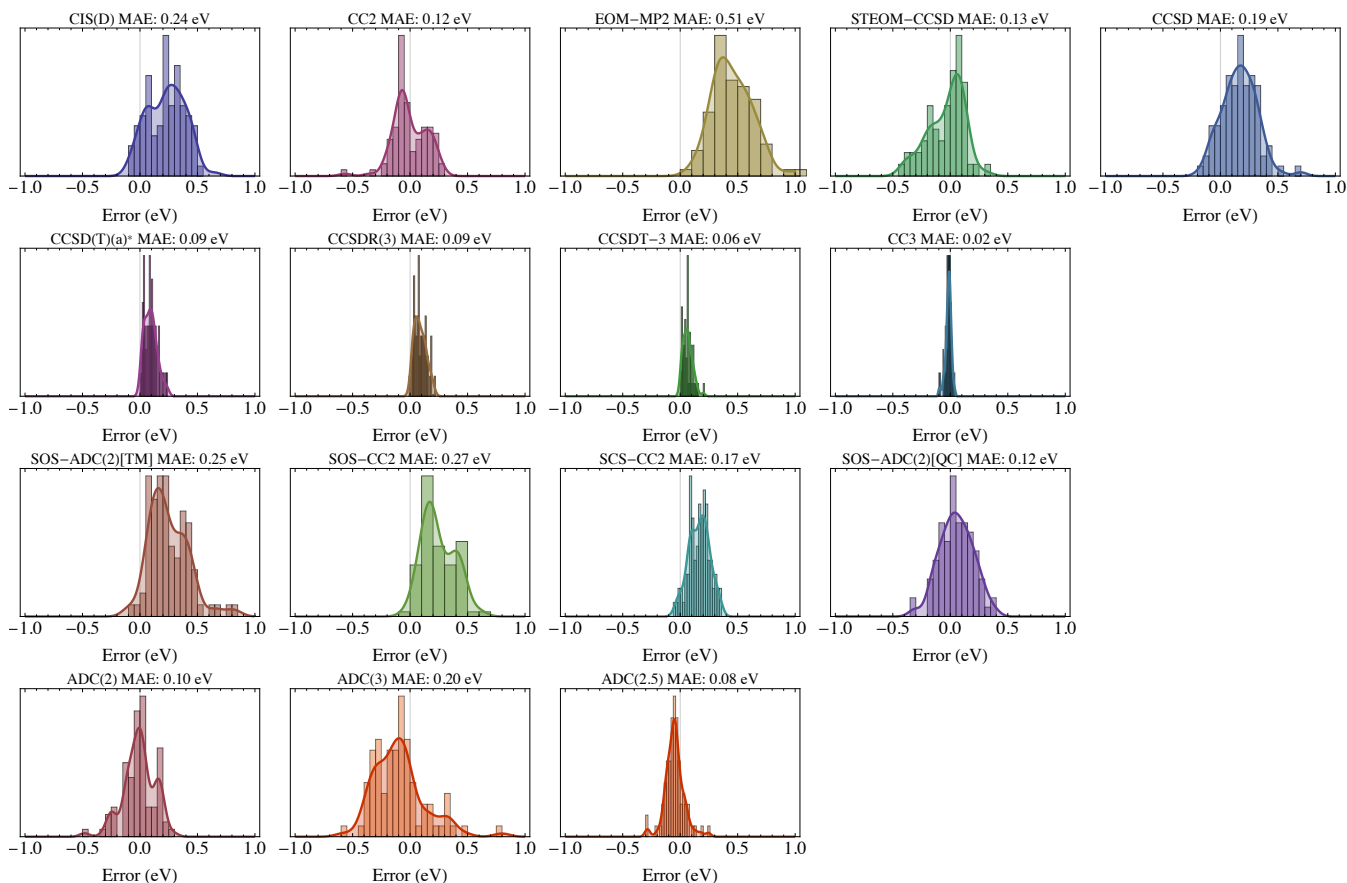


Figure 2: Distribution of the error (in eV) in VTEs (with respect to the TBE/*aug-cc-pVTZ* values) for various methods. See Table 7 for the values of the corresponding statistical quantities. QC and TM indicate that Q-CHEM and TURBOMOLE scaling factors are considered, respectively. The SOS-CC2 and SCS-CC2 approaches are obtained with the latter code

Table 7: Statistical analysis, taking as reference the TBE/*aug-cc-pVTZ* values, for various theoretical models. TM and QC stand for the TURBOMOLE and Q-CHEM definitions of the scaling factors, respectively. On the right-hand side, we compare the MAE obtained here with the previously values obtained for smaller molecules containing 1 to 3 (and 4 to 6) non-hydrogen atoms.<sup>29</sup> All values are in eV.

Method	All states					MAE (subgroup)								MAE (size)		
	Count	MSE	MAE	RMSE	SDE	Sing.	Trip.	Val.	CT	Ryd	$n \rightarrow \pi^*$	$\pi \rightarrow \pi^*$	$\pi \rightarrow \sigma^*$	1-3 at.	4-6 at.	This set
CIS(D)	88	0.23	0.24	0.28	0.16	0.20	0.30	0.27	0.28	0.07	0.28	0.28	0.14	0.23	0.22	0.24
EOM-MP2	91	0.50	0.50	0.60	0.34	0.51	0.48	0.51	0.60	0.36	0.61	0.54	0.54	0.13	0.24	0.50
STEOM-CCSD	63	-0.04	0.13	0.16	0.13	0.09	0.17	0.14	0.06	0.12	0.07	0.18	0.18	0.10	0.12	0.13
CC2	91	0.00	0.12	0.14	0.15	0.11	0.13	0.12	0.11	0.12	0.09	0.13	0.13	0.19	0.15	0.12
SOS-CC2 [TM]	90	0.24	0.24	0.28	0.14	0.24	0.24	0.25	0.27	0.17	0.41	0.17	0.17	0.19	0.23	0.24
SCS-CC2 [TM]	91	0.16	0.16	0.19	0.09	0.15	0.19	0.18	0.17	0.08	0.26	0.15	0.15	0.18	0.17	0.16
ADC(2)	90	-0.01	0.10	0.14	0.13	0.10	0.11	0.11	0.10	0.07	0.12	0.12	0.12	0.19	0.14	0.10
SOS-ADC(2) [TM]	91	0.24	0.25	0.30	0.17	0.28	0.20	0.23	0.25	0.30	0.36	0.15	0.15	0.18	0.21	0.25
SOS-ADC(2) [QC]	91	0.05	0.12	0.15	0.15	0.14	0.09	0.11	0.18	0.11	0.14	0.10	0.10	0.14	0.12	0.12
CCSD	91	0.16	0.18	0.22	0.15	0.23	0.10	0.17	0.29	0.10	0.31	0.15	0.15	0.07	0.13	0.18
ADC(3)	90	-0.10	0.20	0.24	0.22	0.17	0.24	0.21	0.22	0.10	0.21	0.23	0.23	0.24	0.21	0.20
ADC(2.5)	88	-0.05	0.07	0.09	0.08	0.08	0.07	0.07	0.09	0.06	0.06	0.09	0.09	0.10	0.08	0.07
CCSD(T)(a)*	58	0.09	0.09	0.11	0.06	0.09		0.10	0.12	0.05	0.14	0.09	0.09	0.03	0.05	0.09
CCSDR(3)	58	0.09	0.09	0.10	0.06	0.09		0.10	0.11	0.05	0.13	0.08	0.08	0.03	0.05	0.09
CCSDT-3	58	0.06	0.06	0.08	0.05	0.06		0.07	0.08	0.04	0.10	0.06	0.06	0.03	0.05	0.06
CC3	58	-0.02	0.02	0.03	0.02	0.02		0.02	0.03	0.01	0.02	0.03	0.03	0.02	0.01	0.02

ommended for large compounds. In this category, one finds: (i) EOM-MP2, with a MAE quadrupling between the smallest and largest molecules, likely explaining why this method gave reasonable performances in previous works,<sup>141,146</sup> (ii) CCSD with an error steadily increasing from 0.07 to 0.18 eV as the size of the benchmarked compounds increases; and (iii) CCSD(T)(a)\* and CCSDR(3) with MAEs tripling between the smallest and largest molecules, though remaining under the 0.10 eV threshold. While the perturbative triples clearly help in correcting the CCSD VTEs, they are insufficient in order to fully compensate the CCSD overestimations for larger molecules. In the second category of approaches, Table 7 indicates significant improvements of the accuracy as system size increases, i.e., these methods are likely recommendable for “real-life” applications. Both ADC(2) and CC2 belong to this category, with a MAE divided by a factor of two when considering the larger rather than smaller molecules. This trend likely explains the contrasted CC2 results obtained previously when experimental references on large compounds were considered,<sup>136,137,140</sup> or when high-level TBEs on tiny molecules were used<sup>21,26,141</sup> as references. In the last category, one finds approaches that behave relatively similarly for all system size, and this is essentially all the remaining methods.

#### 4. CONCLUDING REMARKS

The vertical transition energies to 91 ESs of bicyclic molecules containing between 8 and 10 non-hydrogen atoms have been evaluated. The selected molecules were chosen to be representative of  $\pi$ -conjugated chromogens actually present in dyes and fluorophores used daily in measurements, e.g., azulene, benzothiadiazole, diketopyrrolopyrrole, quinoxaline, and tetrathiafulvalene. To define our TBEs/*aug-cc-pVTZ* reference values, we typically relied on CC3 for the triplet excited states as they are characterized by a strongly dominant single-excitation character. For the singlet ESs, we employed corrected CC3 VTEs thanks to double- $\zeta$  CCSDT values. Although the present set does not include transitions with a (dominant) double excitation character, it nevertheless includes a reasonable mix of singlet (58), triplet (33), valence (60), Rydberg (17), and CT (13) ESs. Such variety of states is rather typical for molecules of this size, though systems with stronger CT character are missing.<sup>25,105</sup>

Thanks to these TBEs, we have benchmarked 16 wave function methods commonly employed for ES calculations on this type of systems. We stress that the present set considerably extends the number of ESs of “large” molecules (more than 6 non-hydrogen atoms) included in the QUEST database.<sup>29</sup> This allows for a fair evaluation of the performances of various methods as the size of the molecules increases. The outcomes of the present study clearly show that the quality of the VTEs provided by both ADC(2) and CC2 improves with system size, whereas CCSD follows the opposite pathway. In the group of computationally “cheap” models, it seems reasonable to recommend ADC(2), CC2, and STEOM-CCSD. Besides, ADC(2.5) appears as a good compromise to further improve the accuracy: it outperforms the three previous methods almost systematically for a cost equivalent to ADC(3). For the present set, ADC(2.5) deliv-

ers statistical deviations comparable to those obtained with the more resource-intensive CCSD(T)(a)\*, CCSDR(3), and CCSDT-3 approaches, whereas in the case of smaller compounds, the reverse trend was clearly found. Finally, it is probably worth stressing that the present work hints that CC3 delivers excellent accuracies for all treated subsets (ES nature, size of the compounds, etc). While CC3’s  $O(N^7)$  scaling prevents applications on large systems with large basis sets, CC3/double- $\zeta$  calculations are achievable on chromophores, fluorophores, and photochromes of actual practical interest, e.g., substituted naphthoquinones, coumarins, and azobenzenes.

The present results could serve as a reliable guide to select a cheaper level of theory for specific classes of organic compounds. Such a purely theoretical strategy to select a low-scaling theoretical model (e.g., an adequate exchange-correlation functional to perform TD-DFT calculations), on the basis of a straightforwardly accessible property (the vertical transition energy in the present case) can likely be viewed as complementary to the protocols developed by Barone and coworkers in which they model complex spectroscopic properties (such as vibronic spectra) so as to allow direct comparisons with experiment.<sup>147–149</sup>

#### ACKNOWLEDGEMENTS

PFL thanks the European Research Council (ERC) under the European Union’s Horizon 2020 research and innovation programme (grant agreement no. 863481) for financial support. DJ is indebted to the CCIPL computational center installed in Nantes for (the always very) generous allocation of computational time.

#### SUPPORTING INFORMATION AVAILABLE

Raw CCSD/*aug-cc-pVTZ* data. Cartesian coordinates. Theoretical best estimates. VTEs for all benchmarked methods.

#### REFERENCES

- (1) Pople, J. A.; Head-Gordon, M.; Fox, D. J.; Raghavachari, K.; Curtiss, L. A. Gaussian-1 Theory: A General Procedure for Prediction of Molecular Energies. *J. Chem. Phys.* **1989**, *90*, 5622–5629.
- (2) Curtiss, L. A.; Raghavachari, K.; Trucks, G. W.; Pople, J. A. Gaussian-2 Theory for Molecular Energies of First- and Second-row Compounds. *J. Chem. Phys.* **1991**, *94*, 7221–7230.
- (3) Curtiss, L. A.; Raghavachari, K.; Redfern, P. C.; Pople, J. A. Assessment of Gaussian-2 and Density Functional Theories for the Computation of Enthalpies of Formation. *J. Chem. Phys.* **1997**, *106*, 1063–1079.
- (4) Curtiss, L. A.; Raghavachari, K.; Redfern, P. C.; Raszolov, V.; Pople, J. A. Gaussian-3 (G3) Theory for Molecules Containing First and Second-Row Atoms. *J. Chem. Phys.* **1998**, *109*, 7764–7776.
- (5) Curtiss, L. A.; Redfern, P. C.; Raghavachari, K. Gaussian-4 Theory. *J. Chem. Phys.* **2007**, *126*, 084108.
- (6) Sun, J.; Ruzsinszky, A.; Perdew, J. P. Strongly Con-

- strained and Appropriately Normed Semilocal Density Functional. *Phys. Rev. Lett.* **2015**, *115*, 036402.
- (7) Petruzielo, F. R.; Toulouse, J.; Umrigar, C. J. Approaching chemical accuracy with quantum Monte Carlo. *J. Chem. Phys.* **2012**, *136*, 124116.
  - (8) Scemama, A.; Giner, E.; Benali, A.; Loos, P.-F. Taming the fixed-node error in diffusion Monte Carlo via range separation. *J. Chem. Phys.* **2020**, *153*, 174107.
  - (9) Yao, Y.; Giner, E.; Li, J.; Toulouse, J.; Umrigar, C. J. Almost exact energies for the Gaussian-2 set with the semistochastic heat-bath configuration interaction method. *J. Chem. Phys.* **2020**, *153*, 124117.
  - (10) Jurečka, P.; Šponer, J.; Černý, J.; Hobza, P. Benchmark Database of Accurate (MP2 and CCSD(T) Complete Basis Set Limit) Interaction Energies of Small Model Complexes, DNA Base Pairs, and Amino Acid Pairs. *Phys. Chem. Chem. Phys.* **2006**, *8*, 1985–1993.
  - (11) Rezac, J.; Riley, K.; Hobza, P. S66: A Well-Balanced Database of Benchmark Interaction Energies Relevant to Biomolecular Structures. *J. Chem. Theory Comput.* **2011**, *7*, 2427–2438.
  - (12) Tajti, A.; Szalay, P. G.; Császár, A. G.; Kállay, M.; Gauss, J.; Valeev, E. F.; Flowers, B. A.; Vázquez, J.; Stanton, J. F. HEAT: High Accuracy Extrapolated Ab Initio Thermochemistry. *J. Chem. Phys.* **2004**, *121*, 11599–11613.
  - (13) van Setten, M. J.; Caruso, F.; Sharifzadeh, S.; Ren, X.; Scheffler, M.; Liu, F.; Lischner, J.; Lin, L.; Deslippe, J. R.; Louie, S. G.; Yang, C.; Weigend, F.; Neaton, J. B.; Evers, F.; Rinke, P. *GW* 100: Benchmarking  $G_0W_0$  for Molecular Systems. *J. Chem. Theory Comput.* **2015**, *11*, 5665–5687.
  - (14) Stuke, A.; Kunkel, C.; Golze, D.; Todorović, M.; Margraf, J. T.; Reuter, K.; Rinke, P.; Oberhofer, H. Atomic Structures and Orbital Energies of 61,489 Crystal-Forming Organic Molecules. *Sci. Data* **2020**, *7*, 58.
  - (15) Goerigk, L.; Grimme, S. A General Database for Main Group Thermochemistry, Kinetics, and Noncovalent Interactions – Assessment of Common and Reparameterized (meta-)GGA Density Functionals. *J. Chem. Theory Comput.* **2010**, *6*, 107–126.
  - (16) Goerigk, L.; Grimme, S. A Thorough Benchmark of Density Functional Methods for General Main Group Thermochemistry, Kinetics, and Noncovalent Interactions. *Phys. Chem. Chem. Phys.* **2011**, *13*, 6670–6688.
  - (17) Goerigk, L.; Hansen, A.; Bauer, C.; Ehrlich, S.; Najibi, A.; Grimme, S. A Look at the Density Functional Theory Zoo with the Advanced GMTKN55 Database for General Main Group Thermochemistry, Kinetics and Noncovalent Interactions. *Phys. Chem. Chem. Phys.* **2017**, *19*, 32184–32215.
  - (18) Piccardo, M.; Penocchio, E.; Puzzarini, C.; Biczysko, M.; Barone, V. Semi-Experimental Equilibrium Structure Determinations by Employing B3LYP/SNSD Anharmonic Force Fields: Validation and Application to Semirigid Organic Molecules. *J. Phys. Chem. A* **2015**, *119*, 2058–2082.
  - (19) Penocchio, E.; Piccardo, M.; Barone, V. Correction to Semiexperimental Equilibrium Structures for Building Blocks of Organic and Biological Molecules: The B2PLYP Route. *J. Chem. Theory Comput.* **2016**, *12*, 3001–3001.
  - (20) Mendolicchio, M.; Penocchio, E.; Licari, D.; Tasiato, N.; Barone, V. Development and Implementation of Advanced Fitting Methods for the Calculation of Accurate Molecular Structures. *J. Chem. Theory Comput.* **2017**, *13*, 3060–3075.
  - (21) Loos, P.-F.; Scemama, A.; Blondel, A.; Garniron, Y.; Caffarel, M.; Jacquemin, D. A Mountaineering Strategy to Excited States: Highly-Accurate Reference Energies and Benchmarks. *J. Chem. Theory Comput.* **2018**, *14*, 4360–4379.
  - (22) Loos, P.-F.; Boggio-Pasqua, M.; Scemama, A.; Caffarel, M.; Jacquemin, D. Reference Energies for Double Excitations. *J. Chem. Theory Comput.* **2019**, *15*, 1939–1956.
  - (23) Loos, P.-F.; Lipparini, F.; Boggio-Pasqua, M.; Scemama, A.; Jacquemin, D. A Mountaineering Strategy to Excited States: Highly-Accurate Energies and Benchmarks for Medium Size Molecules. *J. Chem. Theory Comput.* **2020**, *16*, 1711–1741.
  - (24) Loos, P.-F.; Scemama, A.; Boggio-Pasqua, M.; Jacquemin, D. A Mountaineering Strategy to Excited States: Highly-Accurate Energies and Benchmarks for Exotic Molecules and Radicals. *J. Chem. Theory Comput.* **2020**, *16*, 3720–3736.
  - (25) Loos, P.-F.; Comin, M.; Blase, X.; Jacquemin, D. Reference Energies for Intramolecular Charge-Transfer Excitations. *J. Chem. Theory Comput.* **2021**, *17*, 3666–3686.
  - (26) Schreiber, M.; Silva-Junior, M. R.; Sauer, S. P. A.; Thiel, W. Benchmarks for Electronically Excited States: CASPT2, CC2, CCSD and CC3. *J. Chem. Phys.* **2008**, *128*, 134110.
  - (27) Silva-Junior, M. R.; Sauer, S. P. A.; Schreiber, M.; Thiel, W. Basis Set Effects on Coupled Cluster Benchmarks of Electronically Excited States: CC3, CCSDR(3) and CC2. *Mol. Phys.* **2010**, *108*, 453–465.
  - (28) Silva-Junior, M. R.; Schreiber, M.; Sauer, S. P. A.; Thiel, W. Benchmarks of Electronically Excited States: Basis Set Effects on CASPT2 Results. *J. Chem. Phys.* **2010**, *133*, 174318.
  - (29) VÉril, M.; Scemama, A.; Caffarel, M.; Lipparini, F.; Boggio-Pasqua, M.; Jacquemin, D.; Loos, P.-F. QUESTDB: a Database of Highly-Accurate Excitation Energies for the Electronic Structure Community. *WIREs Comput. Mol. Sci.* **2021**, *11*, e1517.
  - (30) Huron, B.; Malrieu, J. P.; Rancurel, P. Iterative Perturbation Calculations of Ground and Excited State Energies from Multiconfigurational Zeroth-Order Wavefunctions. *J. Chem. Phys.* **1973**, *58*, 5745–5759.
  - (31) Giner, E.; Scemama, A.; Caffarel, M. Using Perturbatively Selected Configuration Interaction in Quantum Monte Carlo Calculations. *Can. J. Chem.* **2013**, *91*, 879–885.
  - (32) Giner, E.; Scemama, A.; Caffarel, M. Fixed-Node Diffusion Monte Carlo Potential Energy Curve of the Fluorine Molecule  $F_2$  Using Selected Configuration

- Interaction Trial Wavefunctions. *J. Chem. Phys.* **2015**, *142*, 044115.
- (33) Garniron, Y.; Scemama, A.; Loos, P.-F.; Caffarel, M. Hybrid Stochastic-Deterministic Calculation of the Second-Order Perturbative Contribution of Multireference Perturbation Theory. *J. Chem. Phys.* **2017**, *147*, 034101.
- (34) Garniron, Y.; Scemama, A.; Giner, E.; Caffarel, M.; Loos, P.-F. Selected Configuration Interaction Dressed by Perturbation. *J. Chem. Phys.* **2018**, *149*, 064103.
- (35) Garniron, Y.; Applencourt, T.; Gasperich, K.; Benali, A.; Ferté, A.; Paquier, J.; Pradines, B.; As-saraf, R.; Reinhardt, P.; Toulouse, J.; Barbaresco, P.; Renon, N.; David, G.; Malrieu, J.-P.; Véril, M.; Caffarel, M.; Loos, P.-F.; Giner, E.; Scemama, A. Quantum Package 2.0: An Open-Source Determinant-Driven Suite of Programs. *J. Chem. Theory Comput.* **2019**, *15*, 3591–3609.
- (36) Kucharski, S. A.; Bartlett, R. J. Recursive Intermediate Factorization and Complete Computational Linearization of the Coupled-Cluster Single, Double, Triple, and Quadruple Excitation Equations. *Theor. Chim. Acta* **1991**, *80*, 387–405.
- (37) Noga, J.; Bartlett, R. J. The Full CCSDT Model for Molecular Electronic Structure. *J. Chem. Phys.* **1987**, *86*, 7041–7050.
- (38) Scuseria, G. E.; Schaefer, H. F. A New Implementation of the Full CCSDT Model for Molecular Electronic Structure. *Chem. Phys. Lett.* **1988**, *152*, 382–386.
- (39) Kucharski, S. A.; Włoch, M.; Musiał, M.; Bartlett, R. J. Coupled-Cluster Theory for Excited Electronic States: The Full Equation-Of-Motion Coupled-Cluster Single, Double, and Triple Excitation Method. *J. Chem. Phys.* **2001**, *115*, 8263–8266.
- (40) Kowalski, K.; Piecuch, P. The Active-Space Equation-of-Motion Coupled-Cluster Methods for Excited Electronic States: Full EOMCCSDt. *J. Chem. Phys.* **2001**, *115*, 643–651.
- (41) Kowalski, K.; Piecuch, P. Excited-State Potential Energy Curves of CH<sup>+</sup>: a Comparison of the EOM-CCSDt And Full EOMCCSDT Results. *Chem. Phys. Lett.* **2001**, *347*, 237–246.
- (42) Christiansen, O.; Koch, H.; Jørgensen, P. Response Functions in the CC3 Iterative Triple Excitation Model. *J. Chem. Phys.* **1995**, *103*, 7429–7441.
- (43) Koch, H.; Christiansen, O.; Jørgensen, P.; Olsen, J. Excitation Energies of BH, CH<sub>2</sub> and Ne in Full Configuration Interaction and the Hierarchy CCS, CC2, CCSD and CC3 of Coupled Cluster Models. *Chem. Phys. Lett.* **1995**, *244*, 75–82.
- (44) Loos, P. F.; Scemama, A.; Jacquemin, D. The Quest for Highly-Accurate Excitation Energies: A Computational Perspective. *J. Phys. Chem. Lett.* **2020**, *11*, 2374–2383.
- (45) Loos, P.-F.; Jacquemin, D. Is ADC(3) as Accurate as CC3 for Valence and Rydberg Transition Energies? *J. Phys. Chem. Lett.* **2020**, *11*, 974–980.
- (46) Loos, P.-F.; Matthews, D. A.; Lipparini, F.; Jacquemin, D. How Accurate are EOM-CC4 Vertical Excitation Energies? *J. Chem. Phys.* **2021**, *154*, 221103.
- (47) Casanova-Páez, M.; Dardis, M. B.; Goerigk, L.  $\omega$ B2PLYP and  $\omega$ B2GPPLYP: The First Two Double-Hybrid Density Functionals with Long-Range Correction Optimized for Excitation Energies. *J. Chem. Theory Comput.* **2019**, *15*, 4735–4744.
- (48) Casanova-Páez, M.; Goerigk, L. Time-Dependent Long-Range-Corrected Double-Hybrid Density Functionals with Spin-Component and Spin-Opposite Scaling: A Comprehensive Analysis of Singlet–Singlet and Singlet–Triplet Excitation Energies. *J. Chem. Theory Comput.* **2021**, *17*, 5165–5186.
- (49) Mester, D.; Kállay, M. A Simple Range-Separated Double-Hybrid Density Functional Theory for Excited States. *J. Chem. Theory Comput.* **2021**, *17*, 927–942.
- (50) Mester, D.; Kállay, M. Spin-Scaled Range-Separated Double-Hybrid Density Functional Theory for Excited States. *J. Chem. Theory Comput.* **2021**, *17*, 4211–4224.
- (51) Grotjahn, R.; Kaupp, M. Assessment of hybrid functionals for singlet and triplet excitations: Why do some local hybrid functionals perform so well for triplet excitation energies? *J. Chem. Phys.* **2021**, *155*, 124108.
- (52) Hait, D.; Head-Gordon, M. Orbital Optimized Density Functional Theory for Electronic Excited States. *J. Phys. Chem. Lett.* **2021**, *12*, 4517–4529.
- (53) Matthews, D. A.; Cheng, L.; Harding, M. E.; Lipparini, F.; Stopkowitz, S.; Jagau, T.-C.; Szalay, P. G.; Gauss, J.; Stanton, J. F. Coupled-Cluster Techniques for Computational Chemistry: The CFOUR Program Package. *J. Chem. Phys.* **2020**, *152*, 214108.
- (54) Purvis III, G. P.; Bartlett, R. J. A Full Coupled-Cluster Singles and Doubles Model: The Inclusion of Disconnected Triples. *J. Chem. Phys.* **1982**, *76*, 1910–1918.
- (55) Scuseria, G. E.; Scheiner, A. C.; Lee, T. J.; Rice, J. E.; Schaefer, H. F. The Closed-Shell Coupled Cluster Single and Double Excitation (CCSD) Model for the Description of Electron Correlation. A Comparison with Configuration Interaction (CISD) Results. *J. Chem. Phys.* **1987**, *86*, 2881–2890.
- (56) Koch, H.; Jensen, H. J. A.; Jørgensen, P.; Helgaker, T. Excitation Energies from the Coupled Cluster Singles and Doubles Linear Response Function (CCSDLR). Applications to Be, CH<sup>+</sup>, CO, and H<sub>2</sub>O. *J. Chem. Phys.* **1990**, *93*, 3345–3350.
- (57) Stanton, J. F.; Bartlett, R. J. The Equation of Motion Coupled-Cluster Method - A Systematic Biorthogonal Approach to Molecular Excitation Energies, Transition-Probabilities, and Excited-State Properties. *J. Chem. Phys.* **1993**, *98*, 7029–7039.
- (58) Stanton, J. F. Many-Body Methods for Excited State Potential Energy Surfaces. I: General Theory of Energy Gradients for the Equation-of-Motion Coupled-Cluster Method. *J. Chem. Phys.* **1993**, *99*, 8840–8847.
- (59) Frisch, M. J.; Trucks, G. W.; Schlegel, H. B.; Scuseria, G. E.; Robb, M. A.; Cheeseman, J. R.; Scalmani, G.; Barone, V.; Petersson, G. A.; Nakatsuji, H.; Li, X.; Caricato, M.; Marenich, A. V.;

- Bloino, J.; Janesko, B. G.; Gomperts, R.; Men-  
nucci, B.; Hratchian, H. P.; Ortiz, J. V.; Izmaylov, A. F.;  
Sonnenberg, J. L.; Williams-Young, D.; Ding, F.;  
Lipparini, F.; Egidi, F.; Goings, J.; Peng, B.;  
Petroni, A.; Henderson, T.; Ranasinghe, D.; Za-  
krzewski, V. G.; Gao, J.; Rega, N.; Zheng, G.;  
Liang, W.; Hada, M.; Ehara, M.; Toyota, K.;  
Fukuda, R.; Hasegawa, J.; Ishida, M.; Nakajima, T.;  
Honda, Y.; Kitao, O.; Nakai, H.; Vreven, T.;  
Throssell, K.; Montgomery, J. A., Jr.; Peralta, J. E.;  
Ogliaro, F.; Bearpark, M. J.; Heyd, J. J.; Broth-  
ers, E. N.; Kudin, K. N.; Staroverov, V. N.; Keith, T. A.;  
Kobayashi, R.; Normand, J.; Raghavachari, K.; Ren-  
dell, A. P.; Burant, J. C.; Iyengar, S. S.; Tomasi, J.;  
Cossi, M.; Millam, J. M.; Klene, M.; Adamo, C.;  
Cammi, R.; Ochterski, J. W.; Martin, R. L.; Mo-  
rokuma, K.; Farkas, O.; Foresman, J. B.; Fox, D. J.  
Gaussian 16 Revision A.03. 2016; Gaussian Inc.  
Wallingford CT.
- (60) Trofimov, A.; Schirmer, J. Polarization Propagator  
Study of Electronic Excitation in key Heterocyclic  
Molecules I. Pyrrole. *Chem. Phys.* **1997**, *214*, 153–  
170.
- (61) Dreuw, A.; Wormit, M. The Algebraic Diagrammatic  
Construction Scheme for the Polarization Propagator  
for the Calculation of Excited States. *WIREs Comput.  
Mol. Sci.* **2015**, *5*, 82–95.
- (62) Epifanovsky, E.; Gilbert, A. T. B.; Feng, X.;  
Lee, J.; Mao, Y.; Mardirossian, N.; Pokhilko, P.;  
White, A. F.; Coons, M. P.; Dempwolff, A. L.;  
Gan, Z.; Hait, D.; Horn, P. R.; Jacobson, L. D.; Kali-  
man, I.; Kussmann, J.; Lange, A. W.; Lao, K. U.;  
Levine, D. S.; Liu, J.; McKenzie, S. C.; Morri-  
son, A. F.; Nanda, K. D.; Plasser, F.; Rehn, D. R.;  
Vidal, M. L.; You, Z.-Q.; Zhu, Y.; Alam, B.; Al-  
brecht, B. J.; Aldossary, A.; Alguire, E.; Ander-  
sen, J. H.; Athavale, V.; Barton, D.; Begam, K.;  
Behn, A.; Bellonzi, N.; Bernard, Y. A.; Berquist, E. J.;  
Burton, H. G. A.; Carreras, A.; Carter-Fenk, K.;  
Chakraborty, R.; Chien, A. D.; Closser, K. D.;  
Cofer-Shabica, V.; Dasgupta, S.; de Wergifosse, M.;  
Deng, J.; Diedenhofen, M.; Do, H.; Ehlert, S.;  
Fang, P.-T.; Fatehi, S.; Feng, Q.; Friedhoff, T.;  
Gayvert, J.; Ge, Q.; Gidofalvi, G.; Goldey, M.;  
Gomes, J.; González-Espinoza, C. E.; Gulania, S.;  
Gunina, A. O.; Hanson-Heine, M. W. D.; Harbach, P.  
H. P.; Hauser, A.; Herbst, M. F.; Hernández Vera, M.;  
Hodecker, M.; Holden, Z. C.; Houck, S.; Huang, X.;  
Hui, K.; Huynh, B. C.; Ivanov, M.; Jász, Á.; Ji, H.;  
Jiang, H.; Kaduk, B.; Kähler, S.; Khistyayev, K.;  
Kim, J.; Kis, G.; Klunzinger, P.; Koczor-Benda, Z.;  
Koh, J. H.; Kosenkov, D.; Koulias, L.; Kowalczyk, T.;  
Krauter, C. M.; Kue, K.; Kunitsa, A.; Kus, T.; Lad-  
janski, I.; Landau, A.; Lawler, K. V.; Lefrancois, D.;  
Lehtola, S.; Li, R. R.; Li, Y.-P.; Liang, J.; Lieben-  
thal, M.; Lin, H.-H.; Lin, Y.-S.; Liu, F.; Liu, K.-  
Y.; Loipersberger, M.; Luenser, A.; Manjanath, A.;  
Manohar, P.; Mansoor, E.; Manzer, S. F.; Mao, S.-P.;  
Marenich, A. V.; Markovich, T.; Mason, S.; Mau-  
rer, S. A.; McLaughlin, P. F.; Menger, M. F. S. J.;  
Mewes, J.-M.; Mewes, S. A.; Morgante, P.; Mulli-  
nax, J. W.; Oosterbaan, K. J.; Paran, G.; Paul, A. C.;  
Paul, S. K.; Pavošević, F.; Pei, Z.; Prager, S.;  
Proynov, E. I.; Rák, Á.; Ramos-Cordoba, E.; Rana, B.;  
Rask, A. E.; Rettig, A.; Richard, R. M.; Rob, F.;  
Rossomme, E.; Scheele, T.; Scheurer, M.; Schnei-  
der, M.; Sergueev, N.; Sharada, S. M.; Sko-  
morowski, W.; Small, D. W.; Stein, C. J.; Su, Y.-  
C.; Sundstrom, E. J.; Tao, Z.; Thirman, J.; Tor-  
nai, G. J.; Tsuchimochi, T.; Tubman, N. M.; Vec-  
cham, S. P.; Vydrov, O.; Wenzel, J.; Witte, J.;  
Yamada, A.; Yao, K.; Yeganeh, S.; Yost, S. R.;  
Zech, A.; Zhang, I. Y.; Zhang, X.; Zhang, Y.;  
Zuev, D.; Aspuru-Guzik, A.; Bell, A. T.; Besley, N. A.;  
Bravaya, K. B.; Brooks, B. R.; Casanova, D.; Chai, J.-  
D.; Coriani, S.; Cramer, C. J.; Cserey, G.; De-  
Prince, A. E.; DiStasio, R. A.; Dreuw, A.; Duni-  
etz, B. D.; Furlani, T. R.; Goddard, W. A.; Hammes-  
Schiffer, S.; Head-Gordon, T.; Hehre, W. J.; Hsu, C.-  
P.; Jagau, T.-C.; Jung, Y.; Klamt, A.; Kong, J.;  
Lambrecht, D. S.; Liang, W.; Mayhall, N. J.;  
McCurdy, C. W.; Neaton, J. B.; Ochsenfeld, C.;  
Parkhill, J. A.; Peverati, R.; Rassolov, V. A.; Shao, Y.;  
Slipchenko, L. V.; Stauch, T.; Steele, R. P.; Subot-  
nik, J. E.; Thom, A. J. W.; Tkatchenko, A.; Truh-  
lar, D. G.; Van Voorhis, T.; Wesolowski, T. A.; Wha-  
ley, K. B.; Woodcock, H. L.; Zimmerman, P. M.;  
Faraji, S.; Gill, P. M. W.; Head-Gordon, M.; Her-  
bert, J. M.; Krylov, A. I. Software for the frontiers  
of quantum chemistry: An overview of developments  
in the Q-Chem 5 package. *J. Chem. Phys.* **2021**, *155*,  
084801.
- (63) Yanai, T.; Tew, D. P.; Handy, N. C. A New Hybrid  
Exchange-Correlation Functional Using the Coulomb-  
Attenuating Method (CAM-B3LYP). *Chem. Phys.  
Lett.* **2004**, *393*, 51–56.
- (64) Plasser, F.; Wormit, M.; Dreuw, A. New Tools for the  
Systematic Analysis and Visualization of Electronic  
Excitations. I. Formalism. *J. Chem. Phys.* **2014**, *141*,  
024106.
- (65) Plasser, F.; Bäßler, S. A.; Wormit, M.; Dreuw, A.  
New Tools for the Systematic Analysis and Visual-  
ization of Electronic Excitations. II. Applications. *J.  
Chem. Phys.* **2014**, *141*, 024107.
- (66) Le Bahers, T.; Adamo, C.; Ciofini, I. A Qualitative  
Index of Spatial Extent in Charge-Transfer Excitations.  
*J. Chem. Theory Comput.* **2011**, *7*, 2498–2506.
- (67) Adamo, C.; Le Bahers, T.; Savarese, M.; Wilbra-  
ham, L.; García, G.; Fukuda, R.; Ehara, M.; Rega, N.;  
Ciofini, I. Exploring Excited States Using Time De-  
pendent Density Functional Theory and Density-  
Based Indexes. *Coord. Chem. Rev.* **2015**, *304–305*,  
166–178.
- (68) Aidas, K.; Angeli, C.; Bak, K. L.; Bakken, V.; Bast, R.;  
Boman, L.; Christiansen, O.; Cimiraglia, R.; Co-  
riani, S.; Dahle, P.; Dalskov, E. K.; Ekström, U.;  
Enevoldsen, T.; Eriksen, J. J.; Ettenhuber, P.; Fer-  
nández, B.; Ferrighi, L.; Fliegl, H.; Frediani, L.;

- Hald, K.; Halkier, A.; Hättig, C.; Heiberg, H.; Helgaker, T.; Hennum, A. C.; Hetttema, H.; Hjertenæs, E.; Høst, S.; Hoyvik, I.-M.; Iozzi, M. F.; Jansik, B.; Jensen, H. J. A.; Jonsson, D.; Jørgensen, P.; Kauczor, J.; Kirpekar, S.; Kjærgaard, T.; Klopper, W.; Knecht, S.; Kobayashi, R.; Koch, H.; Kongsted, J.; Krapp, A.; Kristensen, K.; Ligabue, A.; Lutnæs, O. B.; Melo, J. I.; Mikkelsen, K. V.; Myhre, R. H.; Neiss, C.; Nielsen, C. B.; Norman, P.; Olsen, J.; Olsen, J. M. H.; Osted, A.; Packer, M. J.; Pawłowski, F.; Pedersen, T. B.; Provasi, P. F.; Reine, S.; Rinkevicius, Z.; Ruden, T. A.; Ruud, K.; Rybkin, V. V.; Sałek, P.; Samson, C. C. M.; de Merás, A. S.; Saue, T.; Sauer, S. P. A.; Schimmelpfennig, B.; Sneskov, K.; Steindal, A. H.; Sylvester-Hvid, K. O.; Taylor, P. R.; Teale, A. M.; Tellgren, E. I.; Tew, D. P.; Thorvaldsen, A. J.; Thogersen, L.; Vahtras, O.; Watson, M. A.; Wilson, D. J. D.; Ziolkowski, M.; Ågren, H. The Dalton Quantum Chemistry Program System. *WIREs Comput. Mol. Sci.* **2014**, *4*, 269–284.
- (69) Head-Gordon, M.; Rico, R. J.; Oumi, M.; Lee, T. J. A Doubles Correction to Electronic Excited States From Configuration Interaction in the Space of Single Substitutions. *Chem. Phys. Lett.* **1994**, *219*, 21–29.
- (70) Head-Gordon, M.; Maurice, D.; Oumi, M. A Perturbative Correction to Restricted Open-Shell Configuration-Interaction with Single Substitutions for Excited-States of Radicals. *Chem. Phys. Lett.* **1995**, *246*, 114–121.
- (71) Stanton, J. F.; Gauss, J. Perturbative Treatment of the Similarity Transformed Hamiltonian in Equation-of-Motion Coupled-Cluster Approximations. *J. Chem. Phys.* **1995**, *103*, 1064–1076.
- (72) Christiansen, O.; Koch, H.; Jørgensen, P. The Second-Order Approximate Coupled Cluster Singles and Doubles Model CC2. *Chem. Phys. Lett.* **1995**, *243*, 409–418.
- (73) Hättig, C.; Weigend, F. CC2 Excitation Energy Calculations on Large Molecules Using the Resolution of the Identity Approximation. *J. Chem. Phys.* **2000**, *113*, 5154–5161.
- (74) Nooijen, M.; Bartlett, R. J. A New Method for Excited States: Similarity Transformed Equation-Of-Motion Coupled-Cluster Theory. *J. Chem. Phys.* **1997**, *106*, 6441–6448.
- (75) Dutta, A. K.; Nooijen, M.; Neese, F.; Izsák, R. Exploring the Accuracy of a Low Scaling Similarity Transformed Equation of Motion Method for Vertical Excitation Energies. *J. Chem. Theory Comput.* **2018**, *14*, 72–91.
- (76) Matthews, D. A.; Stanton, J. F. A new Approach to Approximate Equation-Of-Motion Coupled Cluster with Triple Excitations. *J. Chem. Phys.* **2016**, *145*, 124102.
- (77) Christiansen, O.; Koch, H.; Jørgensen, P. Perturbative Triple Excitation Corrections to Coupled Cluster Singles and Doubles Excitation Energies. *J. Chem. Phys.* **1996**, *105*, 1451–1459.
- (78) Watts, J. D.; Bartlett, R. J. Iterative and Non-Iterative Triple Excitation Corrections in Coupled-Cluster Methods for Excited Electronic States: the EOM-CCSDT-3 and EOM-CCSD( $\tilde{T}$ ) Methods. *Chem. Phys. Lett.* **1996**, *258*, 581–588.
- (79) Prochnow, E.; Harding, M. E.; Gauss, J. Parallel Calculation of CCSDT and Mk-MRCCSDT Energies. *J. Chem. Theory Comput.* **2010**, *6*, 2339–2347.
- (80) Trofimov, A. B.; Stelter, G.; Schirmer, J. Electron Excitation Energies Using a Consistent Third-Order Propagator Approach: Comparison with Full Configuration Interaction and Coupled Cluster Results. *J. Chem. Phys.* **2002**, *117*, 6402–6410.
- (81) Harbach, P. H. P.; Wormit, M.; Dreuw, A. The Third-Order Algebraic Diagrammatic Construction Method (ADC(3)) for the Polarization Propagator for Closed-Shell Molecules: Efficient Implementation and Benchmarking. *J. Chem. Phys.* **2014**, *141*, 064113.
- (82) Neese, F. The ORCA Program System. *WIREs Comput. Mol. Sci.* **2012**, *2*, 73–78.
- (83) Hellweg, A.; Grün, S. A.; Hättig, C. Benchmarking the Performance of Spin-Component Scaled CC2 in Ground and Electronically Excited States. *Phys. Chem. Chem. Phys.* **2008**, *10*, 4119–4127.
- (84) TURBOMOLE V7.3 2018, a development of University of Karlsruhe and Forschungszentrum Karlsruhe GmbH, 1989-2007, TURBOMOLE GmbH, since 2007; available from <http://www.turbomole.com> (accessed 13 June 2016).
- (85) Krauter, C. M.; Pernpointner, M.; Dreuw, A. Application of the Scaled-Opposite-Spin Approximation to Algebraic Diagrammatic Construction Schemes of Second Order. *J. Chem. Phys.* **2013**, *138*, 044107.
- (86) Dierksen, M.; Grimme, S. A Density Functional Calculation of the Vibronic Structure of Electronic Absorption Spectra. *J. Chem. Phys.* **2004**, *120*, 3544–3554.
- (87) Murakami, A.; Kobayashi, T.; Goldberg, A.; Nakamura, S. CASSCF and CASPT2 Studies on the Structures, Transition Energies, and Dipole Moments of Ground and Excited States for Azulene. *J. Chem. Phys.* **2004**, *120*, 1245–1252.
- (88) Falden, H. H.; Falster-Hansen, K. R.; Bak, K. L.; Rettrup, S.; Sauer, S. P. A. Benchmarking Second Order Methods for the Calculation of Vertical Electronic Excitation Energies: Valence and Rydberg States in Polycyclic Aromatic Hydrocarbons. *J. Phys. Chem. A* **2009**, *113*, 11995–12012.
- (89) Huzak, M.; Hajgató, B.; Deleuze, M. Benchmark Theoretical Study of the Ionization Energies, Electron Affinities and Singlet-Triplet Energy Gaps of Azulene, Phenanthrene, Pyrene, Chrysene and Perylene. *Chem. Phys.* **2012**, *406*, 55–64, Single molecule spectroscopy: Current status and perspectives.
- (90) Piecuch, P.; Hansen, J. A.; Staedter, D.; Faure, S.; Blanchet, V. Existence of the Doubly Excited State that Mediates the Photoionization of Azulene. *J. Chem. Phys.* **2013**, *138*, 201102.
- (91) Vosskötter, S.; Konieczny, P.; Marian, C. M.; Weinkauff, R. Towards an Understanding of the

- Singlet–Triplet Splittings in Conjugated Hydrocarbons: Azulene Investigated by Anion Photoelectron Spectroscopy and Theoretical Calculations. *Phys. Chem. Chem. Phys.* **2015**, *17*, 23573–23581.
- (92) Veys, K.; Escudero, D. Computational Protocol To Predict Anti-Kasha Emissions: The Case of Azulene Derivatives. *J. Phys. Chem. A* **2020**, *124*, 7228–7237.
- (93) Gillispie, G. D.; Lim, E. C. Vibrational Analysis of the  $S_2 \rightarrow S_1$  Fluorescence of Azulene in a Naphthalene Mixed Crystal at 4.2 K. *J. Chem. Phys.* **1978**, *68*, 4578–4586.
- (94) Hirata, Y.; Lim, E. C. Radiationless Transitions in Azulene: Evidence for the Ultrafast  $S_2 \rightarrow S_0$  Internal Conversion. *J. Chem. Phys.* **1978**, *69*, 3292–3296.
- (95) Fujii, M.; Ebata, T.; Mikami, N.; Ito, M. Electronic Spectra of Jet-Cooled Azulene. *Chem. Phys.* **1983**, *77*, 191–200.
- (96) Blanchet, V.; Raffael, K.; Turri, G.; Chatel, B.; Girard, B.; Garcia, I. A.; Wilkinson, I.; Whitaker, B. J. Time-Dependent Photoionization of Azulene: Competition Between Ionization and Relaxation in Highly Excited States. *J. Chem. Phys.* **2008**, *128*, 164318.
- (97) Santoro, F.; Jacquemin, D. Going Beyond the Vertical Approximation with Time-Dependent Density Functional Theory. *WIREs Comput. Mol. Sci.* **2016**, *6*, 460–486.
- (98) Fradelos, G.; Lutz, J. J.; Wesolowski, T. A.; Piecuch, P.; Włoch, M. Embedding vs Supermolecular Strategies in Evaluating the Hydrogen-Bonding-Induced Shifts of Excitation Energies. *J. Chem. Theory Comput.* **2011**, *7*, 1647–1666.
- (99) Hollas, J.; Wright, R. Vibrational Analysis of the Near Ultraviolet Spectrum of 2,1,3-Benzothiadiazole and the Analogous Spectra of Benzofurazan and 2,1,3-Benzoselenadiazole. *Spectrochim. Acta A* **1969**, *25*, 1211–1225.
- (100) Prlj, A.; Sandoval-Salinas, M. E.; Casanova, D.; Jacquemin, D.; Corminboeuf, C. Low-Lying  $\pi\pi^*$  States of Heteroaromatic Molecules: A Challenge for Excited State Methods. *J. Chem. Theory Comput.* **2016**, *12*, 2652–2660.
- (101) Refaely-Ambrason, S.; Baer, R.; Kronik, L. Fundamental and Excitation Gaps in Molecules of Relevance for Organic Photovoltaics from an Optimally Tuned Range-Separated Hybrid Functional. *Phys. Rev. B* **2011**, *84*, 075144.
- (102) Lin, T.-S.; Braun, J. R. The Polarized Electronic Spectra and Electric Field Spectra of Benzo-diazoles. II. 2,1,3-Benzothiadiazole. *Chem. Phys.* **1978**, *28*, 379–386.
- (103) Liu, Z.; Wang, X.; Yang, Z.; He, W. Rational Design of a Dual Chemosensor for Cyanide Anion Sensing Based on Dicyanovinyl-Substituted Benzofurazan. *J. Org. Chem.* **2011**, *76*, 10286–10290.
- (104) Li, Y. Molecular Design of Photovoltaic Materials for Polymer Solar Cells: Toward Suitable Electronic Energy Levels and Broad Absorption. *Acc. Chem. Res.* **2012**, *45*, 723–733.
- (105) Kozma, B.; Tajti, A.; Demoulin, B.; Izsák, R.; Nooijen, M.; Szalay, P. G. A New Benchmark Set for Excitation Energy of Charge Transfer States: Systematic Investigation of Coupled Cluster Type Methods. *J. Chem. Theory Comput.* **2020**, *16*, 4213–4225.
- (106) Tsuji, T.; Onoda, M.; Otani, Y.; Ohwada, T.; Nakajima, T.; Hirao, K. Theoretical study on the excited states of heteroarene chromophores: Comparison of calculated and experimental values. *Chem. Phys. Lett.* **2009**, *473*, 196–200.
- (107) Brown, A.; Ngai, T. Y.; Barnes, M. A.; Key, J. A.; Cairo, C. W. Substituted Benzoxadiazoles as Fluorogenic Probes: A Computational Study of Absorption and Fluorescence. *J. Phys. Chem. A* **2012**, *116*, 46–54.
- (108) Chibani, S.; Laurent, A. D.; Le Guennic, B.; Jacquemin, D. Improving the Accuracy of Excited State Simulations of BODIPY and aza-BODIPY Dyes with a Joint SOS-CIS(D) and TD-DFT Approach. *J. Chem. Theory Comput.* **2014**, *10*, 4574–4582.
- (109) Gordon, R.; Yang, R. The Near Ultraviolet Spectra of 2,1,3-Benzothiadiazole and its Deuterated and Substituted Derivatives. *J. Mol. Spectrosc.* **1971**, *39*, 295–320.
- (110) Henry, B. R.; Morrison, J. D. Studies of the Electronic Absorption and Emission Spectra of 2,1,3-Benzothiadiazole. *J. Mol. Spectrosc.* **1975**, *55*, 311–318.
- (111) Chibani, S.; Laurent, A. D.; Blondel, A.; Mennucci, B.; Jacquemin, D. Excited-State Geometries of Solvated Molecules: Going Beyond the Linear-Response Polarizable Continuum Model. *J. Chem. Theory Comput.* **2014**, *10*, 1848–1851.
- (112) Mennucci, B.; Scalmani, G.; Jacquemin, D. Excited-State Vibrations of Solvated Molecules: Going Beyond the Linear-Response Polarizable Continuum Model. *J. Chem. Theory Comput.* **2015**, *11*, 847–850.
- (113) Grzybowski, M.; Gryko, D. T. Diketopyrrolopyrroles: Synthesis, Reactivity, and Optical Properties. *Adv. Opt. Mater.* **2015**, *3*, 280–320.
- (114) Luňák, S.; Vyňuchal, J.; Hrdina, R. Geometry and Absorption of Diketo-pyrrolo-pyrrole Isomers and Their  $\pi$ -Isoelectronic Furo-Furanone Analogues. *J. Mol. Struct.* **2009**, *919*, 239–245.
- (115) McCulloch, I.; Heeney, M.; Chabinyc, M. L.; DeLongchamp, D.; Kline, R. J.; Cöle, M.; Duffy, W.; Fischer, D.; Gundlach, D.; Hamadani, B.; Hamilton, R.; Richter, L.; Salleo, A.; Shkunov, M.; Sparrowe, D.; Tierney, S.; Zhang, W. Semiconducting Thienothiophene Copolymers: Design, Synthesis, Morphology, and Performance in Thin-Film Organic Transistors. *Adv. Mater.* **2009**, *21*, 1091–1109.
- (116) Tasiar, M.; Clermont, G.; Blanchard-Desce, M.; Jacquemin, D.; Gryko, D. T. Synthesis of Bis(arylethynyl)pyrrolo[3,2-b]pyrroles and Effect of Intramolecular Charge Transfer on Their Photophysical Behavior. *Chem. Eur. J.* **2019**, *25*, 598–608.
- (117) Prlj, A.; Curchod, B. F. E.; Fabrizio, A.; Floryan, L.; Corminboeuf, C. Qualitatively Incorrect Features in



- the TDDFT Spectrum of Thiophene-Based Compounds. *J. Phys. Chem. Lett.* **2015**, *6*, 13–21.
- (118) Wu, Y.; Zhu, W. Organic Sensitizers from D- $\pi$ -A to D-A- $\pi$ -A: Effect of the Internal Electron-Withdrawing Units on Molecular Absorption, Energy Levels and Photovoltaic Performances. *Chem. Soc. Rev.* **2013**, *42*, 2039–2058.
- (119) Vuong, T. M. H.; Weimerskirch-Aubatin, J.; Lohier, J.-F.; Bar, N.; Boudin, S.; Labbé, C.; Gourbilleau, F.; Nguyen, H.; Dang, T. T.; Villemin, D. Blue Highly Fluorescent Boron Difluoride Complexes Based on Phthalazine–Pyridine. *New J. Chem.* **2016**, *40*, 6070–6076.
- (120) Shizu, K.; Tanaka, H.; Uejima, M.; Sato, T.; Tanaka, K.; Kaji, H.; Adachi, C. Strategy for Designing Electron Donors for Thermally Activated Delayed Fluorescence Emitters. *J. Phys. Chem. C* **2015**, *119*, 1291–1297.
- (121) Kaito, A.; Hatano, M. Experimental and Theoretical Studies on the Magnetic Circular Dichroism of Azanaphthalenes. Use of the CNDO/S-CI Approximation. *J. Am. Chem. Soc.* **1978**, *100*, 4037–4044.
- (122) Lim, E. C.; Stanislaus, J. Vibronic Perturbations and Phosphorescence of Phthalazine. *J. Chem. Phys.* **1970**, *53*, 2096–2100.
- (123) Innes, K.; Ross, I.; Moomaw, W. R. Electronic States of Azabenzenes and Azanaphthalenes: A Revised and Extended Critical Review. *J. Mol. Spectrosc.* **1988**, *132*, 492–544.
- (124) Mori, H.; Takeshita, K.; Miyoshi, E.; Ohta, N. Theoretical Quest for Photoconversion Molecules Having Opposite Directions of the Electric Dipole Moment in  $S_0$  and  $S_1$  States. *J. Chem. Phys.* **2009**, *130*, 184311.
- (125) Etinski, M.; Marian, C. M. A Theoretical Study of Low-Lying Singlet and Triplet Excited States of Quinazoline, Quinoxaline and Phthalazine: Insight into Triplet Formation. *Phys. Chem. Chem. Phys.* **2017**, *19*, 13828–13837.
- (126) Glass, R. W.; Robertson, L. C.; Merritt, J. A. High-Resolution Electronic Absorption Spectra of Diazanaphthalenes in the Vapor Phase. *J. Chem. Phys.* **1970**, *53*, 3857–3863.
- (127) Nielsen, M. B.; Lomholt, C.; Becher, J. Tetrathiafulvalenes as Building Blocks in Supramolecular Chemistry II. *Chem. Soc. Rev.* **2000**, *29*, 153–164.
- (128) Saito, G.; Yoshida, Y. Development of Conductive Organic Molecular Assemblies: Organic Metals, Superconductors, and Exotic Functional Materials. *Bull. Chem. Soc. Jpn.* **2007**, *80*, 1–137.
- (129) Pou-Amérigo, R.; Ortí, E.; Merchán, M.; Rubio, M.; Viruela, P. M. Electronic Transitions in Tetrathiafulvalene and Its Radical Cation: A Theoretical Contribution. *J. Phys. Chem. A* **2002**, *106*, 631–640.
- (130) Hargittai, I.; Brunvoll, J.; Kolonits, M.; Khodorovsky, V. Tetrathiafulvalene: Gas-Phase Molecular Structure from Electron Diffraction. *J. Mol. Struct.* **1994**, *317*, 273–277.
- (131) Engler, E. M.; Scott, B. A.; Etemad, S.; Penney, T.; Patel, V. V. Organic Alloys: Synthesis and Properties of Solid Solutions of Tetraselenafulvalene-Tetracyano-p-Quinodimethane (TSeF-TCNQ) and Tetrathiafulvalene-Tetracyano-P-Quinodimethane (TTF-TCNQ). *J. Am. Chem. Soc.* **1977**, *99*, 5909–5916.
- (132) Coffen, D. L.; Chambers, J. Q.; Williams, D. R.; Garrett, P. E.; Canfield, N. D. Tetrathioethylenes. *J. Am. Chem. Soc.* **1971**, *93*, 2258–2268.
- (133) Wudl, F.; Kruger, A. A.; Kaplan, M. L.; Hutton, R. S. Unsymmetrical Dimethyltetrathiafulvalene. *J. Org. Chem.* **1977**, *42*, 768–770.
- (134) Electronic spectra of tetrathiafulvalene and its radical cation: analysis of the performance of the time-dependent DFT approach. *Chem. Phys. Lett.* **2002**, *352*, 491–498.
- (135) Kerkines, I. S. K.; Petsalakis, I. D.; Theodorakopoulos, G.; Klopper, W. Low-Lying Absorption and Emission Spectra of Pyrene, 1,6-Dithiaprene, and Tetrathiafulvalene: A Comparison Between ab Initio and Time-Dependent Density Functional Methods. *J. Chem. Phys.* **2009**, *131*, 224315.
- (136) Goerigk, L.; Grimme, S. Assessment of TD-DFT Methods and of Various Spin Scaled CIS<sub>n</sub>D and CC2 Versions for the Treatment of Low-Lying Valence Excitations of Large Organic Dyes. *J. Chem. Phys.* **2010**, *132*, 184103.
- (137) Jacquemin, D.; Duchemin, I.; Blase, X. 0–0 Energies Using Hybrid Schemes: Benchmarks of TD-DFT, CIS(D), ADC(2), CC2, and BSE/GW formalisms for 80 Real-Life Compounds. *J. Chem. Theory Comput.* **2015**, *11*, 5340–5359.
- (138) Hättig, C. In *Response Theory and Molecular Properties (A Tribute to Jan Linderberg and Poul Jørgensen)*; Jensen, H. A., Ed.; Advances in Quantum Chemistry; Academic Press, 2005; Vol. 50; pp 37–60.
- (139) Jacquemin, D. What is the Key for Accurate Absorption and Emission Calculations? Energy or Geometry? *J. Chem. Theory Comput.* **2018**, *14*, 1534–1543.
- (140) Winter, N. O. C.; Graf, N. K.; Leutwyler, S.; Hättig, C. Benchmarks for 0–0 Transitions of Aromatic Organic Molecules: DFT/B3LYP, ADC(2), CC2, SOS-CC2 and SCS-CC2 Compared to High-resolution Gas-Phase Data. *Phys. Chem. Chem. Phys.* **2013**, *15*, 6623–6630.
- (141) Kánnár, D.; Tajti, A.; Szalay, P. G. Accuracy of Coupled Cluster Excitation Energies in Diffuse Basis Sets. *J. Chem. Theory Comput.* **2017**, *13*, 202–209.
- (142) Tajti, A.; Tulipán, L.; Szalay, P. G. Accuracy of Spin-Component Scaled ADC(2) Excitation Energies and Potential Energy Surfaces. *J. Chem. Theory Comput.* **2020**, *16*, 468–474.
- (143) Caricato, M.; Trucks, G. W.; Frisch, M. J.; Wiberg, K. B. Electronic Transition Energies: A Study of the Performance of a Large Range of Single Reference Density Functional and Wave Function Methods on Valence and Rydberg States Compared to Experiment. *J. Chem. Theory Comput.* **2010**, *6*, 370–383.
- (144) Watson, T. J.; Lotrich, V. F.; Szalay, P. G.; Perera, A.; Bartlett, R. J. Benchmarking for Perturbative Triple-

Excitations in EE-EOM-CC Methods. *J. Phys. Chem. A* **2013**, *117*, 2569–2579.

- (145) Kánnár, D.; Szalay, P. G. Benchmarking Coupled Cluster Methods on Valence Singlet Excited States. *J. Chem. Theory Comput.* **2014**, *10*, 3757–3765.
- (146) Tajti, A.; Szalay, P. G. Investigation of the Impact of Different Terms in the Second Order Hamiltonian on Excitation Energies of Valence and Rydberg States. *J. Chem. Theory Comput.* **2016**, *12*, 5477–5482.
- (147) Egidi, F.; Bloino, J.; Cappelli, C.; Barone, V. Development of a Virtual Spectrometer for Chiroptical Spectroscopies: The Case of Nicotine. *Chirality* **2013**, *25*, 701–708.
- (148) Baiardi, A.; Bloino, J.; Barone, V. General Time Dependent Approach to Vibronic Spectroscopy Including Franck–Condon, Herzberg–Teller, and Duschinsky Effects. *J. Chem. Theory Comput.* **2013**, *9*, 4097–4115.
- (149) Baiardi, A.; Bloino, J.; Barone, V. Time-Dependent Formulation of Resonance Raman Optical Activity Spectroscopy. *J. Chem. Theory Comput.* **2018**, *14*, 6370–6390.

# Graphical TOC Entry

